Organometallic Helices: The Mechanism of Formation of "Metallospiralenes"

Jean-Pierre Djukic,*,† Aline Maisse-François,† Michel Pfeffer,*,†
Karl Heinz Dötz,*,‡ André De Cian,§ and Jean Fischer§,||

Laboratoire de Synthèses Métallo-induites, UMR CNRS 7513, Université Louis Pasteur, 4 Rue Blaise Pascal, 67070 Strasbourg, France, Kekulé-Institut für Biochemie und Organische Chemie der Universität Bonn, Gerhard-Domagk Strasse 1, 53171 Bonn, Germany, and Laboratoire de Cristallochimie, UMR CNRS 7513, Université Louis Pasteur, 4 Rue Blaise Pascal, 67070 Strasbourg, France

Received August 9, 2000

A complete investigation of the mechanism of formation of chelated *syn*-facial heterobimetallic benzyl complexes, also referred to as *Cr/Mn-spiralenes*, is presented. Spectroscopic evidence for the intermediacy of a metal carbene species was established by ^{13}C NMR spectroscopy. The nature of the substitution pattern at the carbene carbon atom is shown to play a determining role in the stereoselectivity of spiralene formation. The sequential addition of alkyllithium reagents and MeOTf to a series of cyclomanganated 2-phenylpyridine derivatives afforded mixtures of two isomeric spiralenes, of which a pair of examples has been characterized by X-ray diffraction. The more structurally flexible hetero-bimetallic isomers display an ability to interconvert with the probable mediation of biradical species formed upon homolytic disruption of a benzylic C−Mn bond. Investigation of 2-oxazolinyl derivatives unveiled the origin of the diastereoselective formation of spiralenes. Sequential addition of PhLi and MeOTf to a cyclomanganated 2-[(η^6-4-tolyl)$Cr(CO)_3$]-2-oxazoline derivative afforded a mixture of two products, both resulting from the insertion of a Ph-(MeO)C: moiety into the C_{Ar}−Mn bond. X-ray diffraction analyses reveal that the two compounds are pseudoconformers which differ from the position of the $Mn(CO)_3$ moiety: in one compound, the $Mn(CO)_3$ group is located close to the $Cr(CO)_3$ group, while in the other compound, it is part of a nearly planar six-membered manganacyclic ring coplanar with the π-coordinated arene. These results indicate that in "spiralenes" the helical and spiral-type arrangements are stereoselectively produced if at least one substituent of the transient carbene complex is an aromatic ring capable of electronic interaction with the Mn(I) center during the *cis*-migration process.

Introduction

Construction of molecules with controlled geometry and functional composition is one of the ultimate goals of modern synthetic chemistry.[1] For that purpose criteria such as stereoselectivity and stereospecificity are of extreme importance in transformations that aim at geometrically controlled molecular architectures.[2] Organometallic chemistry has now well demonstrated its strong potential in asymmetric synthesis. As a consequence, sophisticated organometallic complexes, such as some Fischer-type metallacarbenes, increasingly intervene in a stoichiometric fashion, in multistep synthetic schemes as equals of purely organic synthons.[3] With Fischer carbenes, stereoselective transformations arise from those classical effects encountered in organic chemistry as well as from more specific properties of transition metal complexes.[4] We recently reported on the formation of a new class of self-arranged helical chelated (η^3-benzyl)$Mn(CO)_3$ and {η^1[(η^5-cyclohexadienyl)-$Cr(CO)_3$]benzylidene}$Mn(CO)_3$ complexes formed via a putative Fischer-type carbene intermediate.[5] They can

† Laboratoire de Synthèses Métallo-induites, Université Louis Pasteur.
‡ Universität Bonn.
§ Laboratoire de Cristallochimie, Université Louis Pasteur.
|| To whom requests pertaining to X-ray structure determinations should be addressed.

(1) Nicolaou, K. C.; Sorensen, E. J. *Classics in Total Synthesis, Targets, Strategies, Methods*; VCH-Verlag: Weinheim, 1996.
(2) (a) Donovan, R. J. *Chem. Rev.* **1996**, *96*, 635. (b) Tour, J. M. *Chem. Rev.* **1996**, *96*, 537. (c) Shell, A. J. *Chem. Rev.* **1996**, *96*, 195. (d) Ho T.-L. *Stereoselectivity in Organic Synthesis*; Wiley: New York, 1999.
(3) (a) Wulf, W. D. *Comprehensive Organic Synthesis*; Trost, M. M., Flemming, I., Paquette, L. A., Eds.; Pergamon Press: Oxford, 1991; Vol. 5, p 1065. (b) Dötz, K. H.; Straub, W.; Ehlenz, R.; Peseke, K.; Meisel, R. *Angew. Chem., Int. Ed. Engl.* **1995**, *34*, 1856. (c) Dötz, K. H.; Ehlenz, R. *Chem. Eur. J.* **1997**, *3*, 1751. (d) Dötz, K. H.; Klumpe, M.; Nieger, M. *Chem. Eur. J.* **1999**, *5*, 691. (e) Haase, W.-C.; Nieger, M.; Dötz, K. H. *Chem. Eur. J.* **1999**, *5*, 2014. (f) Jäkel, C.; Dötz, K. H. *Tetrahedron* **2000**, *56*, 2167. (g) Merlic, C. A.; Aldrich, C. C.; Albanese-Walker, J.; Saghatelian, A. *J. Am. Chem. Soc.* **2000**, *122*, 3224. (h) Bouaucheau, C.; Parlier, A.; Rudler, H. *J. Org. Chem.* **1997**, *62*, 7247. (i) Su, J.; Wulff, W. D.; Ball, R. G. *J. Org. Chem.* **1998**, *63*, 8440. (j) Quinn, J. F.; Bos, M. E.; Wulff, W. D. *Org. Lett.* **1999**, *1*, 161. (k) Bao, J.; Wulff, W. D.; Fumo, M. J.; Grant, E. B.; Heller, D. P.; Whitcomb, M. C.; Yeung, S. M. *J. Am. Chem. Soc.* **1996**, *118*, 2166. (l) Brown, B.; Hegedus, L. S. *J. Org. Chem.* **2000**, *65*, 1865. (m) Bueno, A. B.; Hegedus, L. S. *J. Org. Chem.* **1998**, *63*, 684. (n) Barluenga, J.; Tomas, M.; Ballesteros, A.; Santamaria, J.; Suarez-Sobrino, A. *J. Org. Chem.* **1997**, *62*, 9229. (o) Aumann, R.; Mayer, A. G.; Fröhlich, R. *J. Am. Chem. Soc.* **1996**, *118*, 10859. (p) Dötz, K. H. *Angew. Chem.* **1975**, *87*, 672; *Angew. Chem., Int. Ed. Engl.* **1984**, *23*, 587. (q) Weyershausen, B.; Dötz, K. H. *Synlett* **1999**, 231. (r) Zaragoza Dörwald, F. *Metal Carbenes in Organic Synthesis*; Wiley-VCH: Weinheim, 1999.

10.1021/om0006920 CCC: $19.00
Publication on Web 11/15/2000

Scheme 1

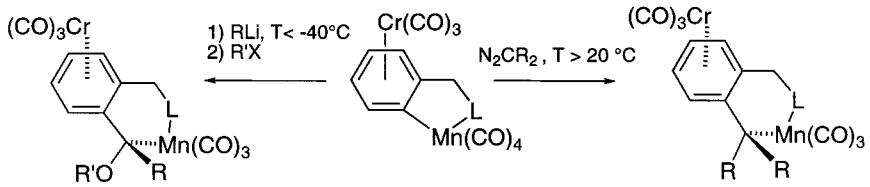

Scheme 2

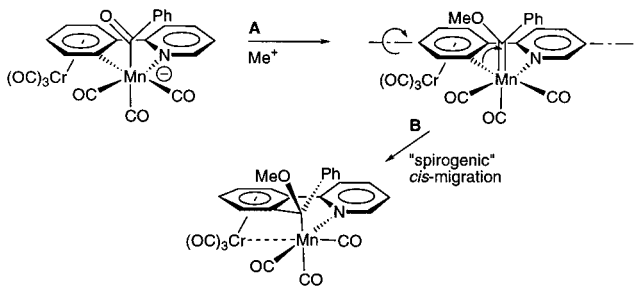

be synthesized by two methods: (1) the sequential treatment of cyclomanganated aromatics of the type *cis*-(L∧C, $\kappa L,\kappa C$)$Mn(CO)_4$ (L∧C = chelating aromatic ligand with L = endogenous two-electron ligand and C = aromatic carbon one-electron ligand) with an aryllithium reagent and MeOTf (the so-called "E. O. Fischer method") at subambient temperatures, (2) the thermolytic reaction of the cyclomanganated substrate with a diazoalkane (Scheme 1).[6]

The recurrent helical shape found in either the monometallic or the bimetallic products motivated us to establish a trivial, albeit sound, terminology. Hence, this novel class of organometallic helical complexes could be accounted for as "spiralenes", as their structures are somewhat reminiscent of spiral staircases in which the metallic core plays the role of a scaffold sustaining an organic "spiral".[7]

We showed that it was possible to control the absolute helicity[8] of the final product by taking advantage of the metallocenic-like planar chirality[9] existing in *ortho*-disubstituted (η^6-arene)$Cr(CO)_3$ substrates bearing a chiral arene substituent. From a mechanistic standpoint, we demonstrated that the nucleophilic attack of a carbonyl ligand attached to Mn (or Re) by RLi was very sensitive to steric hindrance.[10] Cyclomanganated (η^6-arene)$Cr(CO)_3$ complexes would react selectively with PhLi to afford a unique benzoylmanganate complex resulting from the stereoselective addition of the lithiated agent at a Mn (or Re) attached carbonyl ligand located *exo* with respect to the sterically demanding group $Cr(CO)_3$ (Scheme 2, step A). Phenyl-substituted Cr/Mn-spiralenes derived from 2-phenylpyridine display a remarkable inertness to photolytic or thermal treatments with phosphines or CO and possess peculiar structural properties that make them reasonable candidates for nonlinear optical and other photophysical applications.[11]

At this point of our research, we estimated that two crucial issues remained to be further addressed in order to achieve a comprehensive understanding of each of the elementary steps that lead eventually to the typical spiralene's helical arrangements. The first issue was to bring firm evidence for the transient formation of a manganese (or rhenium) carbene species that undergoes the *cis*-migration of the vicinal aryl group leading to the final spiralenes. The second issue was to rationalize the peculiar selectivity with which spiralenes are usually formed when the PhLi/MeOTf sequence is applied (Scheme 2, step B). In all cases, including experiments carried out with mononuclear cyclomanganated aromatics, the phenyl ring originating from PhLi repeatedly ended in the product above the pyridyl group as a consequence of a "spirogenic reaction".[6,12]

We decided to deepen our investigations starting with the hypothesis that such stereoselectivity could arise from a peculiar behavior of the transient carbene species. Herein, we bring forth several elements of answer on the mechanism of formation of spiralenes. We present spectroscopic evidence for the transient formation of a rhenium carbene intermediate upon O-alkylation of a temperature-stable benzoylrhenate complex. We demonstrate that the stereoselectivity observed in the formation of metallospiralenes depends directly upon the nature of the substituents at the carbene carbon and, when applicable, upon the nature

(4) (a) Dötz, K. H.; Tomuschat, P. *Chem. Soc. Rev.* **1999**, *28*, 187. (b) Dötz, K. H.; Pfeiffer, J. *Transition Metals for Organic Synthesis*; Beller, M., Bolm, C., Eds.; Wiley-VCH: Weinheim, 1998; Vol. 1. (c) Gleichmann, M. M.; Dötz, K. H.; Hess, B. A. *J. Am. Chem. Soc.* **1996**, *118*, 10551. (d) Hohmann, F.; Siemoneit, S.; Nieger, M.; Kotila, S.; Dötz, K. H. *Chem. Eur. J.* **1997**, *3*, 853. (d) Dötz, K. H.; Stinner, C. *Tetrahedron Asym.* **1997**, *8*, 1751. (e) Pfeiffer, J.; Dötz, K. H. *Angew. Chem., Int. Ed. Engl.* **1997**, *36*, 2828. (f) Longen, A.; Nieger, M.; Airola, K.; Dötz, K. H. *Organometallics* **1998**, *17*, 1538. (g) Tomuschat, P.; Kröner, L.; Steckhan, E.; Nieger, M.; Dötz, K. H. *Chem. Eur. J.* **1999**, *5*, 700. (h) Weyershausen, B.; Dötz, K. H. *Synlett* **1999**, 231. (i) Ezquerra, J.; Pedregal, C.; Merino, I.; Florez, J.; Barluenga, J.; Garcia-Granda, S.; Llorca, M. A. *J. Org. Chem.* **1999**, *64*, 6554. (k) Barluenga, J.; Bernad, P. L.; Concellon, J. M.; Pinera-Nicolas, A.; Garcia-Granda, S. *J. Org. Chem.* **1997**, *62*, 6870.

(5) (a) Djukic, J. P.; Dötz, K. H.; Pfeffer, M.; De Cian, A.; Fischer, J. *Organometallics* **1997**, *16*, 5171. (b) Djukic, J. P.; Maisse, A.; Pfeffer, M.; Dötz, K. H.; Nieger, M. *Eur. J. Inorg. Chem.* **1998**, 1781. (c) Djukic, J. P.; Maisse, A.; Pfeffer M. *J. Organomet. Chem.* **1998**, *567*, 65.

(6) Djukic, J. P.; Michon, C.; Maisse-François, A.; Allagapen, R.; Pfeffer, M.; Dötz, K. H.; De Cian, A.; Fischer, J. *Chem. Eur. J.* **2000**, *6*, 1064.

(7) From the structure of the final product in Scheme 2 the "organic spiral" consists of the polycyclic organic ligand that is somehow coiled around the C_{benzyl}–Mn bond axis.

(8) Eliel, E. L.; Wilen, S. H. In *Stereochemistry of Organic Compounds*; Wiley: New York, 1994.

(9) Solladié-Cavallo, A. *Adv. Met.-Org. Chem.* **1989**, *1*, 99.

(10) Djukic, J. P.; Maisse, A.; Pfeffer, M.; Dötz, K. H.; Nieger, M. *Organometallics* **1999**, *18*, 2786.

(11) (a) Long, N. J. *Angew. Chem., Int. Ed. Engl.* **1995**, *34*, 21; *Angew. Chem.* **1995**, *107*, 37. (b) Dorn, R. D.; Baums, D.; Kersten, P.; Regener, R. *Adv. Mater.* **1992**, *4*, 464. (c) Whittall, I. R.; McDonagh, A. M.; Humphrey, M. G.; Samoc, M. *Adv. Organomet. Chem.* **1998**, *42*, 291. (d) Whittall, I. R.; McDonagh, A. M.; Humphrey, M. G.; Samoc, M. *Adv. Organomet. Chem.* **1999**, *43*, 349. (e) Eaton, D. F.; Meredith, G. R.; Miller, J. S. *Adv. Mater.* **1991**, *3*, 564. (f) Manners, I. *J. Chem. Soc., Chem. Commun.* **1999**, 857. (g) Kalyanasundaran, K.; Grätzel, M. *Coord. Chem. Rev.* **1998**, *177*, 127. (h) Lees, A. J. *Coord. Chem. Rev.* **1998**, *177*, 3. (i) Stufkens, D. J.; Vlcek, A. *Chem. Rev.* **1998**, 127. (j) Lees, A. J. *Chem. Rev.* **1987**, *87*, 711.

(12) A "spirogenic" reaction denotes a transformation that favors the formation of molecular helical and spiral-like arrangements among all other possible structures.

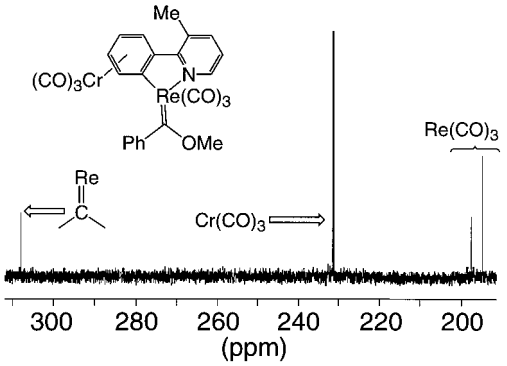

Figure 1. ^{13}C {^1H}NMR spectrum of **3** in CD_2Cl_2 (125 MHz). Enlargement of the 310−190 ppm region.

Scheme 3

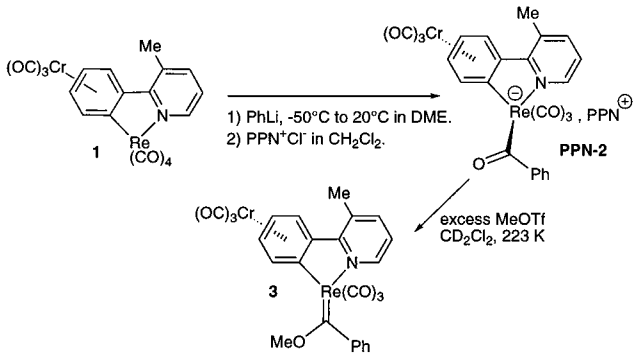

of the organolithium reagent used for the formation of the acylmetalate adduct. Moreover, we propose a mechanistic scheme that rationalizes the formation of spiralenes obtained from cyclomanganated aromatics by the "E.O. Fischer method".

Results and Discussion

1. Spectroscopic Evidence for the Intermediacy of a Rhenium (I)−Carbene Species in the Synthesis of a Cr(0)/Re(I)-Spiralene. 1.1. Spectroscopic Detection of the [(Methoxy)(phenyl)methylidene]-rhenium(I) Species 3. We recently underlined the synthetic versatility of the acylmanganate salts obtained from a reaction of RLi with a cyclomanganated (η^6-arene)$Cr(CO)_3$ complex, as they could be valuable intermediates for the synthesis of *ortho* acyl-substituted (η^6-arene)$Cr(CO)_3$ complexes.[10] We described the X-ray diffraction structure of the rhenium analogue **2** that confirmed the stereoselectivity of the nucleophilic attack of PhLi at the $Re(CO)_4$ fragment of **1** (Scheme 3). Hence, we undertook to monitor by ^{13}C NMR spectroscopy the reaction between an excess amount of MeOTf and the PPN salt of the benzoylrhenate **2**, e.g., PPN-**2** (Scheme 3). The reaction was carried out by injecting MeOTf in an NMR sample tube containing a CD_2Cl_2 solution of PPN-**2** at −50 °C. Complete conversion of PPN-**2** into the neutral carbene complex **3** took place in approximately 1 h (Scheme 3).

A large series of scans were then acquired at −50 °C in order to obtain a ^{13}C NMR spectrum of the carbene intermediate with an acceptable signal-to-noise ratio. The latter spectrum displayed a series of typical signals in the carbonyl ligand resonance region (Figure 1). The carbene carbon signal showed up at δ = 308 ppm, a value typical for neutral Re carbene complexes.[13] The ^{13}C signal of the $Cr(CO)_3$ moiety appeared at a value of δ = 231 ppm, which corresponds to a shielding of 6 ppm with respect to the value extracted from the spectrum of PPN-**2**. This shielding of the ^{13}C signals of $Cr(CO)_3$ is consistent with a decrease of electron density at the Cr atom[14] that is caused by the electron-demanding alkoxycarbene moiety at the Re atom. It is well established that electronic effects of arene's substituent(s), i.e., inductive and mesomeric effects, are readily transmitted to the CO ligands via the coordinated aromatic ring.[15] In addition, it may reasonably be proposed that the shielding of the ^{13}C signal of the Cr-bound CO ligands is caused by a decrease of the d−π* back-donation from the chromium toward the carbonyls and an increase of the σ-donation of the latter.[16]

Warming the NMR sample tube to room temperature induced a rapid change in the solution's content that was characterized by the disappearance of the signal at δ = 308 ppm and the formation of a new major product that was later identified as Cr/Re-spiralene complex **4**.

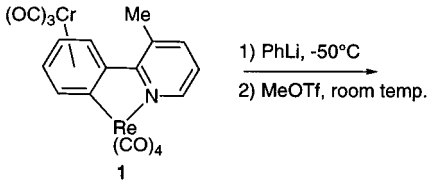

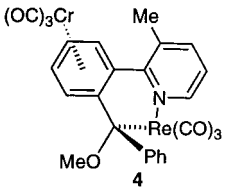

(1)

1.2. Synthesis of Cr/Re-Spiralene 4. The synthesis of complex **4** was carried out on larger scales by starting from the bimetallic complex **1** (eq 1). The latter was treated sequentially with PhLi and MeOTf at −50 °C in DME, and the product, **4**, was recovered in 51% yield after chromatographic purification. Recrystallization of **4** from a mixture of CH_2Cl_2 and hexane afforded crystals suitable for X-ray diffraction analyses.

The ORTEP diagram of the molecular structure of **4** is displayed in Figure 2. Acquisition and refinement data are listed in Table 1. Selected interatomic distances and angles are given in Table 2. The structure of **4**

(13) (a) Darst, K. P.; Lenhert, P. G.; Lukehart, C. M.; Warfield, L. T. *J. Organomet. Chem.* **1980**, *195*, 317. (b) Singh, M. M.; Angelici, R. J. *Inorg. Chem.* **1984**, *23*, 2699. (c) Alvarez-Toledano, C.; Parlier, A.; Rudler, M.; Daran, J. C.; Knobler, C.; Jeannin, Y. *J. Organomet. Chem.* **1987**, *328*, 357. (d) Miessler, G. L.; Kim, S.; Jacobson, R. A.; Angelici, R. J. *Inorg. Chem.* **1987**, *26*, 1690. (e) Casey, C. P.; Nagashima, H. *J. Am. Chem. Soc.* **1989**, *111*, 2352. (f) Casey, C. P.; Sakoba, H.; Underiner, T. L. *J. Am. Chem. Soc.* **1991**, *113*, 6673. (g) Mashima, K.; Jyodol, K.; Ohyoshi, A.; Takaya, H. *Bull. Chem. Soc. Jpn.* **1991**, *64*, 2065.

(14) Fedorov, L. A.; Petrovskii, P. V.; Fedin, E. I.; Panosyan, G. A.; Tsoi, A. A.; Baranetskaya, N. K.; Setkina, V. N. *J. Organomet. Chem.* **1979**, *182*, 499.

(15) (a) Neuse, E. W. *J. Organomet. Chem.* **1975**, *99*, 287. (b) Hunter, A. D.; Shilliday, L.; Furey, W. S.; Zaworotko, M. J. *Organometallics* **1992**, *11*, 1550. (c) Hunter, A. D.; Mozol, V.; Tsai, S. D. *Organometallics* **1992**, *11*, 2251. (d) Djukic, J. P.; Rose-Munch, F.; Rose, E.; Vaissermann, J. *Eur. J. Inorg. Chem.* **2000**, 1295.

(16) Ruiz-Morales, Y.; Schreckenbach, G.; Ziegler, T. *J. Phys. Chem.* **1996**, *100*, 3359.

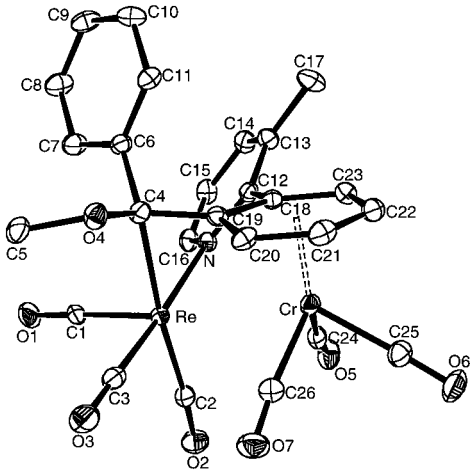

Figure 2. ORTEP diagram of the structure of **4**. Thermal ellipsoids are drawn at the 30% probability level. Solvent and hydrogen atoms have been omitted for clarity.

presents several similarities to those of previously described bimetallic Cr/Mn-spiralenes. The phenyl ring originating from PhLi is typically located above the pyridyl group, thus generating $\pi-\pi$ contacts in the area where interplanar distances are inferior to 3.6 ± 0.1 Å (Table 2).[17] Noteworthy, the Cr−Re distance of 3.080(3) Å in **4** is slightly longer than in the Mn analogue although remaining in the range of values reported by us in several previous cases. The main difference between Mn and Re analogues arises from the conformational behavior of the $Cr(CO)_3$ tripod.[18] In complex **4** studied at 283 K, the ^{13}C (125 MHz) nuclei of the slowly rotating $Cr(CO)_3$ group resonate as three distinct and sharp signals, while in the Mn isomer complete decoalescence may be observed only starting from 253 K.[19] This suggests that a tiny variation of ca. 0.1 Å of the atomic radius of the atom M (M = Mn or Re) connected to the benzylic position in a Cr/M-spiralene complex induces changes of the conformational behavior of the $Cr(CO)_3$ tripod. According to our previous investigations on the conformational behavior of the $Cr(CO)_3$ rotor in Cr/Mn-spiralenes,[19] we may reasonably ascribe the relative slackening in **4** essentially to an increased steric interaction of the Cr-centered rotor with the vicinal $M(CO)_3$ (M = Re) group generated by a decreased molecular flexibility.

The intriguing stereoselectivity observed in the formation of spiralenes from the reactions carried out by the "E.O. Fischer method" prompted us to investigate the outlet of sequential reactions that would involve alkyllithium nucleophiles such as *n*-BuLi and MeLi knowing that the latter are either efficient bases capable of removing aryl protons from (η^6-arene)$Cr(CO)_3$ complexes[20] or capable of attacking unsaturated N-heterocycles.[21]

2. Alkyl-Substituted Cr(0)/Mn(I)-Spiralenes. 2.1. Sequential Reaction of Cyclomanganated 3-Methyl,2-[tricarbonyl(η^6-phenyl)chromium]pyridine, 5, with *n*-BuLi and MeOTf. Addition of a stoichiometric amount of *n*-BuLi to complex **5** in DME at −50 °C afforded a dark brown solution that was subsequently treated with a slight excess of MeOTf and warmed at room temperature. The resulting mixture of products (76% conversion) was separated by chromatographic means to yield two dark red compounds, **6a** and **6b**, in a ratio of 38:62 (eq 2, R = Me). Both complexes afforded crystals that allowed X-ray diffraction analyses. Compounds **6a** and **6b** were subsequently identified as two new Cr/Mn-spiralene complexes in which, for **6a**, a *n*-Bu group was located above the heterocyclic ring at the *endo* position (Figure 3) and, for **6b**, the methoxy group was located above the pyridyl fragment while the *n*-Bu group stood at the *exo* position (Figure 4).

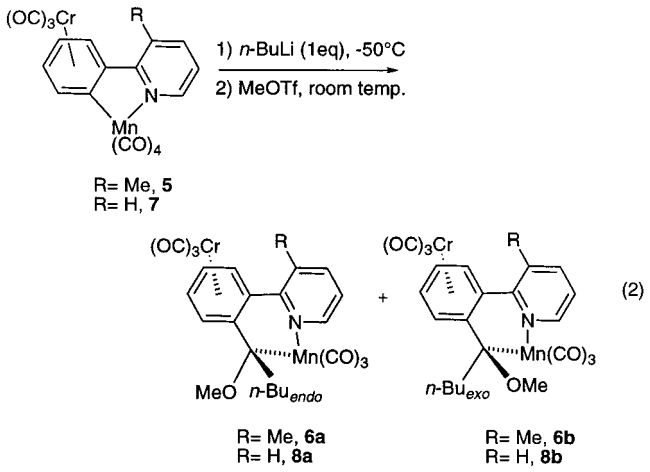

Acquisition and refinement parameters for structures of **6a** and **6b** are provided in Table 1. Selected interatomic distances and angles are given in Table 3. The two ORTEP diagrams of compounds **6a** and **6b** indicate that these *syn*-facial bimetallic isomers possess very close structural features. The stereochemical differences existing between these two diastereoisomers at the benzylic carbon position can also be revealed by ^1H NMR spectroscopy. Indeed, the chemical shift of the methoxy group protons singlet may be used as a probe for determining the spatial position of the latter group relative to the heterocyclic ring; in **6a** as well as in other phenyl-substituted Cr/Mn-spiralene complexes the *exo*-methoxy group protons resonate as a singlet around 3.6 ppm, while in **6b** the same protons which are now located directly in the shielding cone of the pyridyl group resonate at about 3.0 ppm. Complexes **6a** and **6b** are both formed following a process that includes the *cis*-migration of the π-coordinated arene to a α-methoxy-*n*-pentylidene moiety. In view of these results, the absence of unsaturation at α and β positions from the

(17) For leading references please see: (a) Dahl, T. *Acta Chem. Scand.* **1994**, *48*, 95. (b) Hunter, C. A. *Chem. Soc. Rev.* **1994**, 101. (c) Müller-Dethlefs, K.; Hobza, P. *Chem. Rev.* **2000**, *100*, 143.

(18) McGlinchey M. J. *Adv. Organomet. Chem.* **1992**, *34*, 285, and references therein.

(19) Djukic, J. P.; Pfeffer, M.; Dötz, K. H. *C. R. Acad. Sci. Paris, Ser. IIc* **1999**, 403.

(20) (a) Semmelhack, M. F. *Comprehensive Organometallic Chemistry II*; Abel, E. W., Stone, F. G. A., Wilkinson, G., Eds.; Pergamon: Oxford, 1995; Vol. 9, p 1117. (b) Nesmeyanov, A. N.; Kolobova, N. E.; Anisimov, K. N.; Markarov, Yu. V. *Izv. Akad. Nauk. SSSR, Ser. Khim.* **1969**, 2665. (c) Fraser, R. R.; Mansour, T. S. *J. Organomet. Chem.* **1986**, *310*, C60. (d) Ghavshou, M.; Widdowson, D. A. *J. Chem. Soc., Perkin Trans. 1* **1983**, 3065. (e) Semmelhack, M. F.; Bisaha, J.; Czarny, M. *J. Am. Chem. Soc.* **1979**, *101*, 768. (f) Card, R. J.; Trahanovski, W. S. *J. Org. Chem.* **1980**, *45*, 2560. (g) Uemura, M.; Nishikawa, N.; Take, K.; Ohnishi, M.; Hirotsu, K.; Higushi, T.; Hayashi, Y. *J. Org. Chem.* **1983**, *48*, 2349. (h) Rose-Munch, F.; Rose, E. *Current Org. Chem.* **1999**, *3*, 445.

(21) Oae, S.; Furukawa, N. *Adv. Heterocycl. Chem.* **1990**, *48*, 35.

Table 1. Acquisition and Refinement Data for Complexes 4, 6a, 6b, 9, 18, and 19

	4	6a	6b
formula	$C_{26}H_{18}CrNO_7Re{\cdot}CH_2Cl_2$	$C_{24}H_{22}NO_7CrMn$	$2(C_{24}H_{22}NO_7CrMn){\cdot}H_2O{\cdot}CH_2Cl_2$
mol wt	779.57	543.38	1189.71
cryst syst	monoclinic	monoclinic	triclinic
space group	$P2_1/n$	$P2_1/n$	$P\bar{1}$
a (Å)	9.5566(2)	10.1444(3)	9.1890(2)
b (Å)	13.7631(3)	14.3587(3)	12.9030(4)
c (Å)	20.9170(5)	16.4887(6)	13.0610(4)
α (deg)			62.701(7)
β (deg)	101.106(2)	92.744(9)	76.915(7)
γ (deg)			76.943(7)
V (Å^3)	2699.7(2)	2399.0(2)	1327(7)
Z	4	4	1
color	orange	orange	orange
cryst dimens (mm)	0.20 × 0.18 × 0.14	0.20 × 0.15 × 0.11	0.20 × 0.12 × 0.10
ρ_{calcd} (g·cm^{-3})	1.92	1.50	1.49
μ (mm^{-1})	5.127	0.989	1.001
temp (K)	173	294	173
λ (Å)	0.71073	0.71073	0.71073
radiation	Mo Kα graphite monochromated	Mo Kα graphite monochromated	Mo Kα graphite monochromated
diffractometer	KappaCCD	KappaCCD	KappaCCD
hkl limits	0,13/0,18/−29,29	0,12/0,17/−20,20	0,12/−15,17/−16,16
θ limits (deg)	2.5/30.53	2.5/26.37	2.5/29.55
number of data measd	19 975	18 113	11 668
number of data with $I > 3\sigma(I)$	6892	3108	4279
weighting scheme	$4F_o^2/(\sigma^2(F_o^2) + 0.0064F_o^4)$	$4F_o^2/(\sigma^2(F_o^2) + 0.0064F_o^4)$	$4F_o^2/(\sigma^2(F_o^2) + 0.0064F_o^4)$
no. of variables	352	307	343
R	0.035	0.034	0.047
R_w	0.051	0.049	0.075
GOF	1.015	1.020	1.525
largest peak in final diff (e·Å^{-3})	0.703	0.389	0.464

	9	18	19
formula	$C_{28}H_{32}CrMnNO_7$	$C_{26}H_{22}CrMnNO_8$	$C_{26}H_{22}CrMnNO_8$
mol wt	601.50	583.40	583.40
cryst syst.	orthorhombic	monoclinic	monoclinic
space group	$P2_12_12_1$	$P2_1/c$	$P2_1/c$
a (Å)	10.4149(3)	20.2330(7)	15.3920(7)
b (Å)	16.1127(3)	16.5760(3)	10.8910(5)
c (Å)	16.8256(5)	16.9120(5)	14.8720(5)
α (deg)			
β (deg)		114.618(4)	91.030(2)
γ (deg)			
V (Å^3)	2823.5(2)	5156.4(6)	2492.7(3)
Z	4	8	4
color	dark red	red	orange
cryst. dimens (mm)	0.18 × 0.16 × 0.12	0.20 × 0.20 × 0.08	0.16 × 0.14 × 0.10
ρ_{calcd} (g·cm^{-3})	1.41	1.50	1.55
μ (mm^{-1})	0.877	0.961	0.994
temp (K)	173	294	173
λ (Å)	0.71073	0.71073	0.71073
radiation	Mo Kα graphite monochromated	Mo Kα graphite monochromated	Mo Kα graphite monochromated
diffractometer	KappaCCD	KappaCCD	KappaCCD
hkl limits	−10,14/−20,17/−23,16	0,23/0,21/−28,26	0,19/−13,14/−19,19
θ limits (deg)	2.5/30.54	2.5/30.52	2.5/27.55
no. of data meas.	18 579	34 497	17 357
number of data with $I > 3\sigma(I)$	3163	7921	7294
weighting scheme	$4F_o^2/(\sigma^2(F_o^2) + 0.0001F_o^4)$	$4F_o^2/(\sigma^2(F_o^2) + 0.0064F_o^4)$	$4F_o^2/(\sigma^2(F_o^2) + 0.0064F_o^4)$
no. of variables	343	667	334
R	0.034	0.040	0.044
R_w	0.041	0.059	0.083
GOF	0.924	1.108	1.509
largest peak in final diff (e·Å^{-3})	0.330	0.307	0.801

carbene carbon atom clearly affects the stereoselectivity of the process leading to alkyl-substituted bimetallic spiralenes.

2.2. Sequential Reaction of Cyclomanganated 2-[Tricarbonyl(η^6-phenyl)chromium]pyridine, 7, with RLi (R = *n*-Bu, Me) and MeOTf. Sequential treatment of the bimetallic chelate **7** with stoichiometric amounts of *n*-BuLi and MeOTf at −50 °C afforded a new mixture of two compounds that were identified according to ^{1}H NMR investigations as being Cr/Mn-spiralene complexes **8a** and **8b** in a ratio of 48:52 (eq 2, R = H). The latter two compounds displayed spectroscopic features similar to those of **6a** and **6b**. The stoichiometry of the first step of the preparation, e.g., the nucleophilic

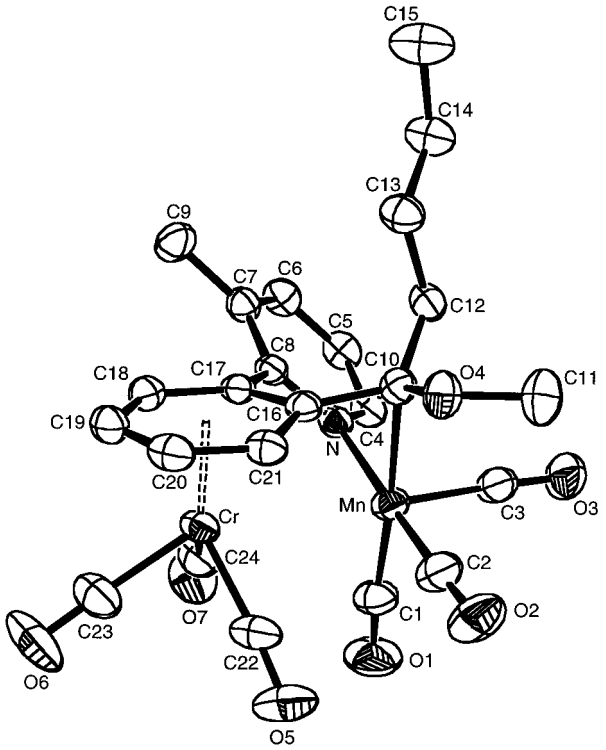

Figure 3. ORTEP diagram of the structure of **6a**. Thermal ellipsoids are drawn at the 40% probability level. Hydrogen atoms have been omitted for clarity.

Table 2. Selected Interatomic Distances (Å), Angles (deg), and Torsion Angles (deg) for Complex 4

Distances (Å)	
Re−Cr	3.080(3)
Re−C4	2.269(3)
Re−C18	3.090(3)
Re−C19	2.601(3)
Cr−C18	2.237(3)
Cr−C19	2.345(4)
Cr−C20	2.228(3)
Cr−C21	2.214(4)
Cr−C22	2.197(3)
Cr−C23	2.222(3)
C4−C19	1.459(4)
Angles (deg)	
C24−Cr−C25	81.8(2)
C24−Cr−C26	97.7(2)
C25−Cr−C26	83.7(2)
Torsion Angle (deg)	
C19−C18−C12−N	47.6
Inter-ring Distances (Å)	
C6−N	3.054
C6−C13	3.553
C11−C12	3.334

attack of RLi, was found to be crucial. We found that reaction of **7** with 2 equiv of *n*-BuLi followed by a treatment with excess MeOTf would yield a unique new product (55% yield) having nothing in common with **8a** and **8b** according to the spectroscopic data (Scheme 4).

This new complex, **9**, was successfully crystallized and characterized by X-ray diffraction analysis. Acquisition and refinement data are listed in Table 1. Complex **9** crystallized spontaneously in the noncentrosymmetric space group $P2_12_12_1$ (the Flack parameter is given in the Experimental Section). Selected interatomic distances and angles are given in Table 4. The structure

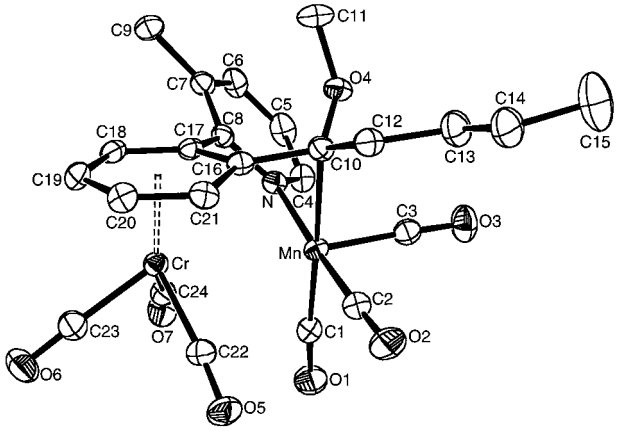

Figure 4. ORTEP diagram of the structure of **6b**. Thermal ellipsoids are drawn at the 40% probability level. Solvent and hydrogen atoms have been omitted for clarity.

Table 3. Selected Interatomic Distances (Å) and Angles (deg) for Complexes 6a and 6b

	6a	6b
Distances (Å)		
Mn−Cr	3.035(4)	3.018(4)
Mn−C10	2.157(3)	2.132(3)
Mn−C16	2.396(4)	2.416(4)
Mn−C17	2.922(4)	2.939(4)
Cr−C16	2.413(3)	2.388(4)
Cr−C17	2.246(2)	2.251(3)
Cr−C18	2.196(3)	2.212(3)
Cr−C19	2.190(3)	2.192(3)
Cr−C20	2.211(3)	2.215(3)
Cr−C21	2.239(3)	2.238(3)
C10−C16	1.446(4)	1.457(4)
Angles (deg)		
C22−Cr−C23	82.4(2)	82.5(2)
C22−Cr−C23	93.4(1)	94.2(1)
C23−Cr−C24	85.2(1)	82.6(2)
C12−C10−O4	110.7(2)	
Torsion Angles (deg)		
C16−C17−C8−N	46.6	45.8

Scheme 4

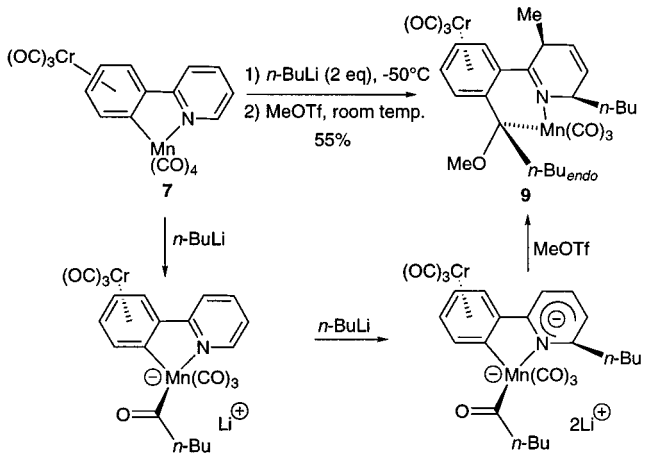

of **9** (Figure 5) reveals that substrate **7** underwent two successive nucleophilic attacks of *n*-BuLi, the first one occurring at a Mn-bound CO ligand and the second one at the 6 position of the pyridyl group, i.e., atom C20 in Figure 5 (Scheme 4). The methyl group connected to C17 originates from MeOTf as a result of the C-alkylation of a putative dianionic intermediate. Strikingly, the two alkyl groups, *n*-Bu and Me, selectively attacked the

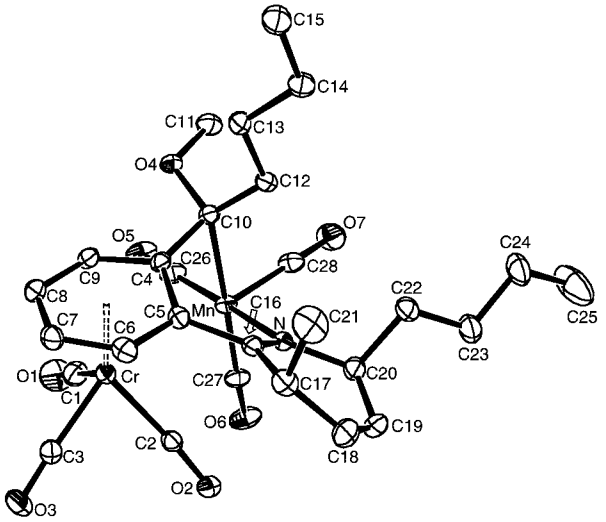

Figure 5. ORTEP diagram of the structure of **9**. Thermal ellipsoids are drawn at the 40% probability level. Hydrogen atoms have been omitted for clarity.

Table 4. Selected Interatomic Distances (Å) and Angles (deg) for Complex 9

Distances (Å)		Angles (deg)	
Mn−Cr	3.060(4)	C1−Cr−C2	95.0(2)
Mn−C4	2.338(4)	C1−Cr−C3	87.1(2)
Mn−C5	2.881(4)	C2−Cr−C3	81.6(2)
Mn−C10	2.148(4)		
Cr−C4	2.422(4)		
C4−C10	1.443(5)		
N−C16	1.290(5)		
C18−C19	1.327(7)		

pyridyl ring from the side opposite the $Cr(CO)_3$ tripod. A rough analysis of the molecular geometry of **9** reveals a "boat"-type conformation for the 1,4-dihydropyridyl group. Further applications of this new reaction are under investigation.

Complexes **8a** and **8b** in solution displayed a peculiar ability to interconvert within a few hours period (eq 3). We never observed this behavior with the relatively rigid phenyl-substituted Cr/Mn-spiralenes. The study of the equilibration between **8a** and **8b** could be followed by monitoring the ^{1}H NMR signal of the relevant methoxy groups of the two latter complexes. Two parallel experiments were carried out by dissolving mixtures enriched in either **8a** or **8b** in $CDCl_3$ at room temperature; three spectra were measured at $t = 0$, 24, 48 h. Table 5 gives the composition of the corresponding solutions at each time interval; experiment 1 corresponds to the isomerization of **8a** into **8b** + **8a** and experiment 2 to the isomerization of **8b** into **8a** + **8b**. Within experimental errors, the two experiments led after 24 h to a rough 50:50 mixture of **8a** and **8b**.

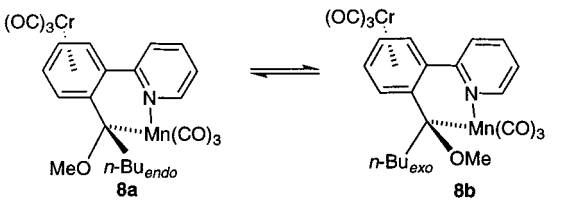

(3)

It is worth noting that such a fluxional behavior was not observed with **6a** and **6b**. The isomerization of **8a** into **8b** corresponds to a formal permutation of the substituents of the benzylic carbon, which is chemically possible, in our opinion, only after homolytic cleavage of the C_{benzyl}−Mn bond[22] and a subsequent 180° rotation of the (*n*-Bu)(MeO)C− fragment around the C_{benzyl}−$C_{ipso/ArCr}$ axis. This would imply the transient formation of a dissymmetric biradical species in which the unpaired electrons are formally located at the Mn atom and at the benzylic position and more probably delocalized over all the surrounding ligands.[23] An ESR experiment that was carried out with a frozen solution of **8a** in degassed $CDCl_3$ supports the hypothesis of a mediation by a biradical species as relatively weak, broad, and complex ESR signals were recorded at ca. $g = 2.02$ and 2.77 (see Supporting Information). The lack of resolution in the latter spectrum may be ascribed to the inherent complexity of the system, i.e., short ESR T_1 and T_2 relaxation times and complex superimposition of signals resulting from classical hyperfine couplings and spin−orbit interaction(s) between the two intramolecularly unpaired electrons. A priori, the strongest signal at $g = 2.02$ may be related to either carbon or a Mn(0)-centered radicals.[24] Further investigations are currently in progress to understand the origin of the second signal.

Table 5. Equilibration of 8a and 8b: Composition of the Reaction Medium (mol %) versus Time (h)

	experiment 1		experiment 2	
t (h)	**8a** (mol %)	**8b** (mol %)	**8a** (mol %)	**8b** (mol %)
0	93	7	15	85
24	56	44	51	49
48	56	44	51	49

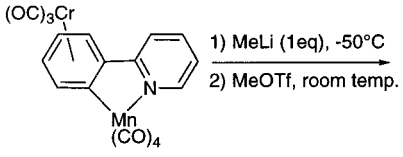

7

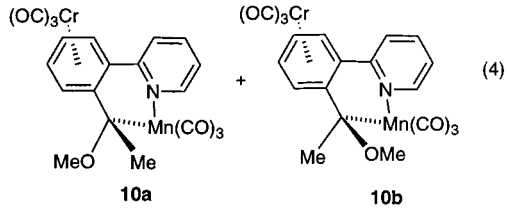

(4)

Aiming at molecules that would possess a higher fluxionality, we decided to attempt the preparation of complexes **10a** and **10b** by treatment of **7** with a stoichiometric amount of MeLi and a slight excess of

(22) (a) Tyler, D. R. *Prog. Inorg. Chem.* **1988**, *36*, 125. (b) Brown, T. L. *Organometallic Radical Processes, Journal of Organometallic Chemistry Library 32*; Trogler, W. C., Ed.; Elsevier: Amsterdam, 1990; p 67.

(23) For reviews on organometallic radicals see: (a) Connelly, N. G.; Geiger, W. E. *Adv. Organomet. Chem.* **1984**, *23*, 1. (b) Sun, S.; Sweigart, D. *Adv. Organomet. Chem.* **1996**, *40*, 171.

(24) (a) Ran, S.; Cheng, C. P. *J. Chem. Soc., Dalton Trans.* **1988**, 2695. (b) Milukov, V. A.; Sinyashin, O. G.; Ginzburg, A. G.; Kondratenko, M. A.; Loim, N. M.; Gubskaya, V. P.; Musin, R. Z.; Morozov, V. I.; Batyeva, E. S.; Sokolov, V. I. *J. Organomet. Chem.* **1995**, *493*, 221. (c) Mach, K.; Novakova, J.; Raynor, J. B. *J. Organomet. Chem.* **1992**, *439*, 341. (d) Symons, M. C. R.; Sweany, R. L. *Organometallics* **1982**, *1*, 834. (d) Rattinger, G. B.; Belford, R. L.; Walker, H.; Brown, T. L. *Inorg. Chem.* **1989**, *28*, 1059. (e) Myers, R. J. *Molecular Magnetism and Magnetic Resonance Spectroscopy*; Prentice Hall: London, 1973.

MeOTf. The latter reactions carried out from −50 to −10 °C afforded a crude mixture of the two expected compounds in which **10b** was the minor component (less than 7%) (eq 4). The moderate conversion obtained for this reaction (33%) suggests either that the products displayed some sensitivity to air or that the acylmanganate intermediate did not completely O-alkylate. The major product, **10a**, was carefully purified by flash column chromatography at −5 °C and was firmly identified on the basis of the ^{1}H chemical shifts of the MeO and Me groups, which showed up respectively at $\delta = 3.69$ and 1.75 ppm. Although complex **10b** could be formed by allowing **10a** to isomerize at room temperature in CH_2Cl_2, it could not be isolated in a pure form. A qualitative ^{1}H NOESY two-dimensional NMR experiment revealed a set of cross-peaks between the ^{1}H NMR signals of **10a** and **10b**, thus confirming that the two latter compounds were undergoing interconversion in solution (eq 5).

10a ⇌ **10b** (5)

The ^{1}H NMR spectrum of **10b** displayed two resonances at $\delta = 2.91$ and 2.03 ppm ascribed to the *endo*-MeO and *exo*-Me groups, respectively. Compounds **10a**,**b** were found more reactive and air sensitive than **8a**,**b**. From a practical point of view, we noticed that the isomerization of **10a** into **10b** was more convenient to monitor by NMR spectroscopy than that of a **8a** + **8b** mixture since the complexity of the ^{1}H NMR spectrum was very much reduced for the former in the 0−4 ppm region.

2.3. Fluxional Behavior of the Alkyl-Substituted Cr/Mn-Spiralene 10a. Complex **10a** and an exact amount of internal standard, e.g., tris-1,3,5-*tert*-butylbenzene, were dissolved in dry and degassed C_6D_6. The resulting dark brown solution was injected in a NMR sample tube that was introduced in the probe of the NMR spectrometer and kept at 293 K. The isomerization of **10a** into **10b** was monitored by ^{1}H NMR spectroscopy. The relative concentrations of **10a** and **10b** were calculated from the integrations of the signals of MeO and Me groups of the two complexes relative to those of the internal standard ($c_{standard} = 0.0124$ M). The concentrations of **10a** and **10b** were summed and compared with the initial concentration of **10a** in order to evaluate the extent of the competing decomposition process that could involve both **10a** and **10b**. The values of ($c_{\mathbf{10a}} + c_{\mathbf{10b}}$) plotted versus time (not shown herein) indicated that the process could be followed over 5 h without noticeable decomposition taking place.

Figure 6 displays the plot of the concentration in **10b**, $c_{\mathbf{10b}}$ (mmol·L^{-1}), versus time (min). The data could be satisfactorily fitted ($R = 0.99951$) with a first-order kinetic law corresponding to the relaxation of an out-of-equilibrium two-component system: $c_{\mathbf{10b}} = c_{\mathbf{10b}}^{e} \times (1 - \exp[-t/(k_1 + k_{-1})])$ with $c_{\mathbf{10b}}^{e} = 6.18 \times 10^{-3}$ M. By extrapolation, the value of the concentration in **10a** at equilibrium, $c_{\mathbf{10a}}^{e}$, could be determined as equal to 20.88×10^{-3} M. The value of the equilibrium constant $K = k_1 \times (k_{-1})^{-1} = c_{\mathbf{10b}}^{e} \times (c_{\mathbf{10a}}^{e})^{-1}$ determined to be 0.42 indicates that the interconverting system favors the isomer in which steric interactions with the pyridyl group are minimized, e.g., **10a**.[25] Figure 7 displays the plot of $\ln[(c_{\mathbf{10b}}^{e} - c_{\mathbf{10b}}) \times (c_{\mathbf{10b}}^{e})^{-1}]$ versus time (min). The curve was fitted to a least-squares linear equation,

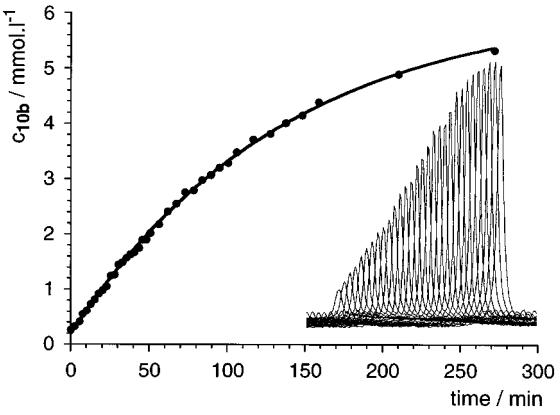

Figure 6. Conversion of **10a** into **10b**; plot of the concentration of **10b** (mmol·L^{-1}) versus time (min). The inset displays the evolution of the ^{1}H NMR signal of the benzylic carbon bound Me group in **10b** versus time.

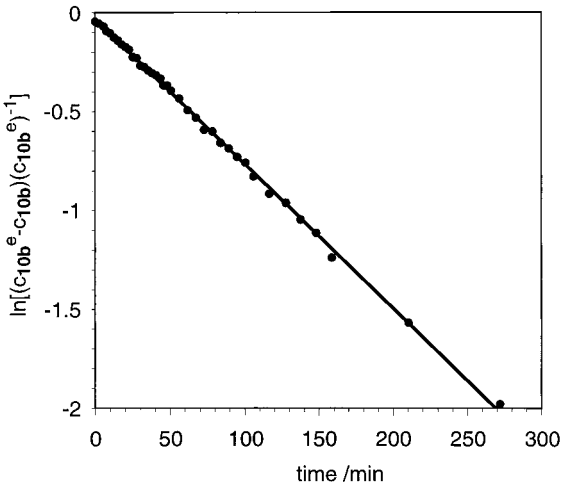

Figure 7. Conversion of **10a** into **10b**; plot of $\ln[(c_{\mathbf{10b}}^{e} - c_{\mathbf{10b}})(c_{\mathbf{10b}}^{e})^{-1}]$ versus time (min).

which allowed the determination of the direct and reverse apparent rate constants: $k_1 = 3.6 \times 10^{-5}$ s^{-1}, $k_{-1} = 8.60 \times 10^{-5}$ s^{-1} ($R = 0.99944$). However, the first-order kinetic law that is used here to extract the apparent rate constants does not reflect the actual mechanism of the conversion of **10a** into **10b**. It seems likely that this reversible process involves a three-step mechanism that includes (i) the slow homolytic cleavage of the C_{benzyl}−Mn bond and the subsequent formation of radicals at the (η^6-benzyl)Cr(CO)$_3$[26] and Mn(CO)$_3$L fragments (Scheme 5, step A), (ii) the slow rotation of the Me(MeO)C− fragment around the C_{benzyl}−C_{Ar} axis, which is expected to occur with a relatively high energy barrier since a part of the spin density is expected to be transferred to the "hermaphroditic" Cr(CO)$_3$ moiety,[27] thus increasing the double-bond character (Scheme 5,

(25) A similar study carried out at +40 °C indicated that the equilibrium was reached in ca. 6 min and that significant decomposition was starting after 15 min; the two complexes **10a** and **10b** were estimated to be in a respective ratio of 4:1 at $t = 6$ min ($K = 0.25$).

(26) (a) Schmaltz, H. G.; Siegel, S.; Bats, J. W. *Angew. Chem., Int. Ed. Engl.* **1995**, *34*, 2383. (b) Taniguchi, N.; Kaneta, N.; Uemura, M. *J. Org. Chem.* **1996**, *61*, 6088. (c) Taniguchi, N.; Uemura, M. *Synlett* **1997**, 51. (d) Taniguchi, N.; Uemura, M. *Tetrahedron Lett.* **1997**, *38*, 7199. (e) Merlic, C. A.; Walsh, J. C. *Tetrahedron Lett.* **1998**, *39*, 2083. (f) Schmaltz, H. G.; Siegel, S.; Bernicke, D. *Tetrahedron Lett.* **1998**, *39*, 6683. (g) Schmaltz, H. G.; de Koning, C. B.; Bernicke, D.; Siegel, S.; Pfletschinger, A. *Angew. Chem., Int. Ed. Engl.* **1999**, *38*, 1620.

Scheme 5

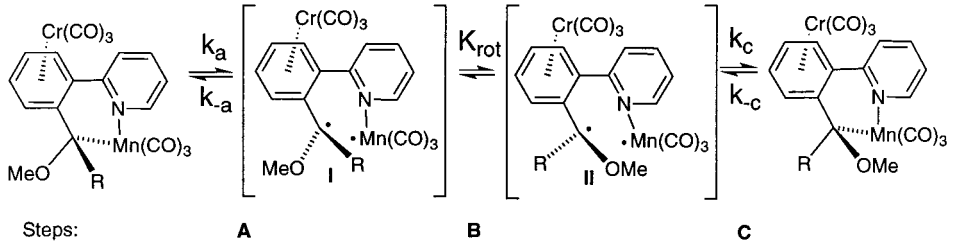

$$K = K_{rot}\,[(k_a \times k_c)/(k_{-c} \times k_{-a})]$$

Scheme 6

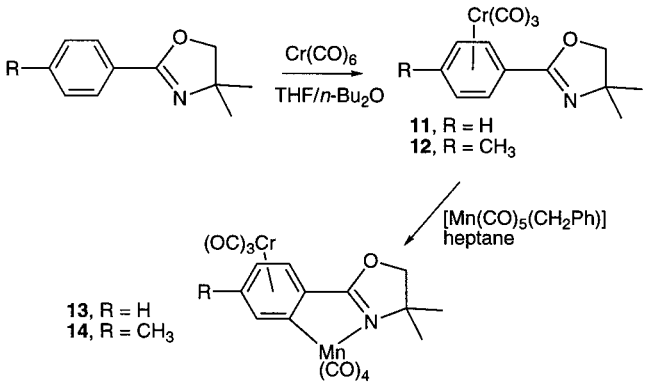

step B), (iii) the fast recombination of the biradical to form a new C_{benzyl}–Mn bond (Scheme 5, step C).

For such a system that implies successive reversible steps there exists unfortunately no straightforward formulation of the complete kinetic law. Nevertheless, it can be easily demonstrated that, at equilibrium, the value of the equilibrium constant K directly depends on the conformational equilibrium constant K_{rot} involving the two biradical species **I** and **II** (Scheme 5). This is further verified if one assumes that the cleavage (k_a, k_{-c}) and recombination (k_{-a}, k_c) rate constants have similar magnitudes. The equilibrium constant K can then be assimilated to K_{rot} (Scheme 5).

In other cases where such conformational exchange and homolytic C_{benzyl}–Mn bond cleavage do not proceed either for steric or electronic reasons, like with **6a**,**b** and with other Cr/Mn(Re)-spiralene complexes having a Ph group attached to the benzylic position, the observed high stereoselectivity of the *cis*-migration step that precedes spiralene formation very likely stems from a late transition state and/or a transient intermediate that prefigures the structure of the final product. The study of bimetallic chelates derived from 2-aryl-2-oxazoline brought us decisive elements for the establishment of the main factors that control the stereoselectivity.

3. 2-Oxazoline-Derived Substrates and Cr(0)/Mn(I) Heterobimetallic Complexes. 3.1. Reactivity of 13 and 14 versus Organolithium and Diazoalkane Reagents. Chromium complexes **11** and **12** afforded in satisfactory yields complexes **13** and **14** respectively upon treatment with $[Mn(CO)_5(CH_2Ph)]$ in refluxing heptane (Scheme 6).

Complex **13** displayed a reactivity versus MeLi similar to that of the 2-phenylpyridine and *N*,*N*-dimethylbenzylamine analogues.[10] Reaction of **13** with a slight excess of MeLi in DME at −50 °C afforded a dark brown solution, which yielded the aromatic ketone **15** in 86% yield upon warming the medium to room temperature and exposing it to air (eq 6).

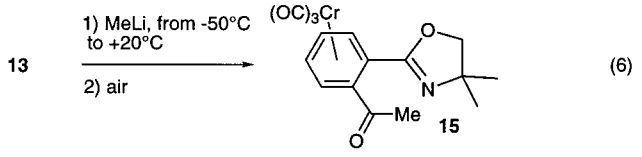

(6)

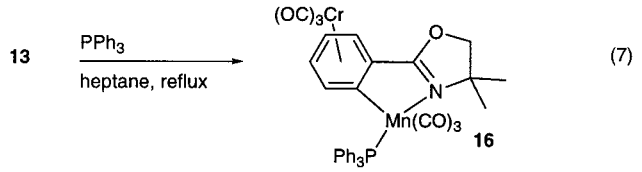

(7)

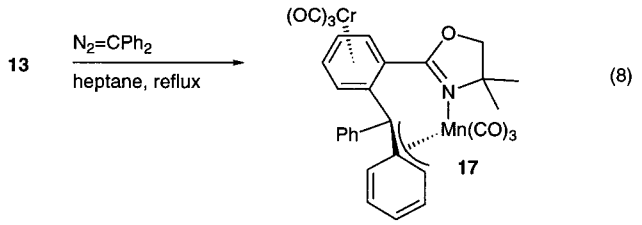

(8)

Complex **13** reacted readily with PPh_3 in refluxing heptane to yield **16**, a new complex resulting from the displacement of the *exo* axial CO ligand of the $Mn(CO)_4$ moiety (eq 7).[6] The relative lability of **13** prompted us to treat it with $N_2{=}CPh_2$, which was expected to yield a new *syn*-facial heterobimetallic Cr/Mn-spiralene with an oxazoline chelating arm (eq 8). The product of the reaction, i.e., **17**, afforded at 263 K a ^{13}C NMR spectrum that suggested that the $Cr(CO)_3$ tripod was not undergoing restricted rotation since its ^{13}C nuclei generated a unique sharp singlet. The ^{13}C signals of the carbonyl ligands connected to the manganese(I) atom were detected at values of chemical shift that suggested that the chelated $Mn(CO)_3$ moiety was not located in the vicinity of the $Cr(CO)_3$ group but was rather engaged in the η^2 coordination of one of the two phenyl groups attached to the benzylic carbon. Indeed, in *syn*-facial bimetallic complexes—or Cr/Mn-spiralenes—the $Mn(CO)_3$ fragment generates three distinct ^{13}C NMR signals at approximately $\delta = 230$, 229, and 220 ppm,[5b] while in chelated η^3-benzylic complexes—or Mn-spiralenes—the resonances related to $Mn(CO)_3$ appear at $\delta = 230$, 221, and 220 ppm.[5a] Our hypothesis for a non-*syn*-facial bimetallic structure was further supported by the IR spectrum of **17** that displayed a *fac*-$Mn(CO)_3$-

(27) (a) Pfletschinger, A.; Dargel, T. K.; Schmaltz, H. G.; Koch, W. *Chem. Eur. J.* **1999**, *5*, 537. (b) Merlic, C. A.; Walsh, J. C.; Tantillo, D. J.; Houk, K. N. *J. Am. Chem. Soc.* **1999**, *121*, 3596.

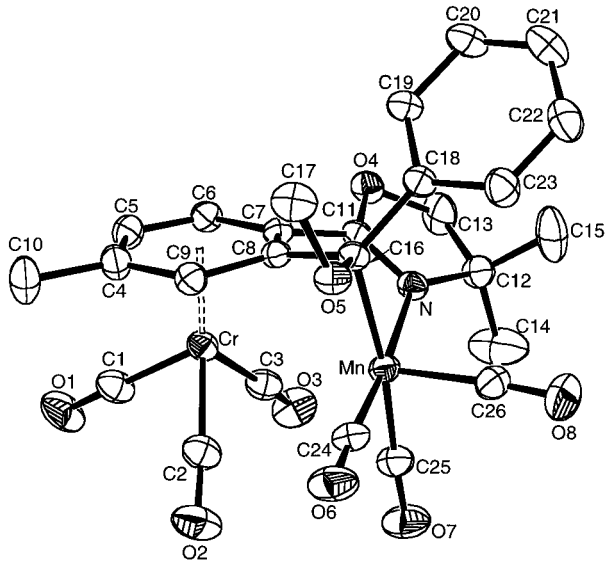

Figure 8. ORTEP diagram of the structure of **18**. Thermal ellipsoids are drawn at the 40% probability level. Hydrogen atoms have been omitted for clarity.

related stretching A-mode vibration band at 2004 cm^{-1}, while it usually appears in *syn*-facial heterobimetallic complexes 5−10 cm^{-1} higher at around 2010−2015 cm^{-1}.[5b]

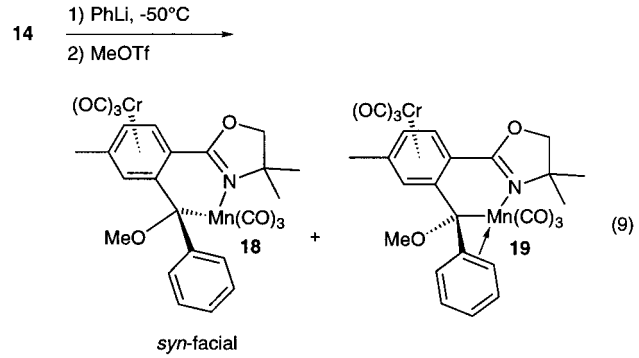

3.2. Sequential Reaction of 14 with PhLi and MeOTf. Our procedure for the synthesis of 2-phenylpyridine-derived Cr/Mn-spiralenes was applied to complex **14** with PhLi as nucleophile and MeOTf as alkylating agent. The experiment afforded a mixture of two new compounds of brown and bright orange color, respectively, that could be separated only by recrystallization and hand sorting of the crystals (eq 9). Recrystallization of the crude mixture indicated that the orange complex was the minor component of the solid mixture. A rough ratio of 15:1 could be established by comparison of the respective weights of the brown and orange crystals. Crystals of acceptable quality of both **18** and **19** were submitted to X-ray diffraction analyses.

Complexes **18** and **19** were thus undoubtedly identified as products both resulting from the insertion of a (phenyl)(methoxy)methylidene unit in the C_{Ar}−Mn bond of **14**. Acquisition and refinement parameters for **18** and **19** are listed in Table 1. Selected interatomic distances and angles are given in Table 6. The ORTEP diagram representing complex **18** (Figure 8) clearly shows the *syn*-facial relationship between the two metal centers. The intermetallic distance of 3.137(5) Å that is longer than in Cr/Mn-spiralenes derived from 2-phenylpyridine[5b] invalidates the existence of an efficient metal−metal bonding interaction. The phenyl ring introduced by PhLi eclipses the bulky 4,4-dimethyl,2-oxazoline heterocycle. One of the two methyl groups of the latter ring (C15) points toward the centroid of the phenyl group, leading us to suspect the existence of a stabilizing intramolecular C−H···π interaction.[28] Observation of the molecular structure of **18** suggests at first glance that this complex is a geometrically locked conformer of **19** resulting from the rocking of the $Mn(CO)_3$ group toward the $Cr(CO)_3$ moiety. The molecular structure of **19** (Figure 9) differs from that of **18** by the position of the Mn center with respect to the π-coordinated aromatic ligand. In **19**, the Mn atom is ideally positioned in the mean plane formed by C16, C8, C7, C11, and N, which is nearly coplanar with the vicinal π-coordinated arene and the oxazoline rings. The interatomic distances C16−Mn, C18−Mn, and C19−Mn reveal that the manganese atom is bonded to C16 and C18−C19 respectively in η^1 and η^2 coordination modes. The molecular structure of **19** displays an example of a nearly planar six-membered metalacycle from which the planarity is ensured by three fused rings, namely, the chromium-complexed arene ring at C7−C8, the 2-oxazolinyl group at N−C11, and the four-membered manganacycle formed by Mn, C16, C18, C19 at Mn−C16.

Surprisingly, solution ^1H NMR investigations of a mixture of **18** and **19** did not afford satisfactory results.

Table 6. Selected Interatomic Distances (Å) and Angles (deg) for Complexes 18 and 19

	18	**19**
	Distances (Å)	
Mn−Cr	3.137(5)	4.887(4)
Mn−C8	2.474(5)	
Mn−C16	2.133(3)	2.130(3)
Mn−C18		2.242(3)
Mn−C19		2.355(3)
Cr−C4	2.232(3)	2.246(3)
Cr−C5	2.205(3)	2.229(3)
Cr−C6	2.227(3)	2.193(3)
Cr−C7	2.219(3)	2.214(2)
Cr−C8	2.377(5)	2.277(3)
Cr−C9	2.215(3)	2.228(3)
C8−C16	1.459(4)	1.510(4)
C16−C18	1.508(4)	1.489(4)
C18−C19	1.385(4)	1.428(4)
C19−C20	1.391(5)	1.414(4)
C20−C21	1.368(5)	1.374(4)
C21−C22	1.381(5)	1.406(5)
C22−C23	1.368(5)	1.375(5)
C23−C18	1.404(4)	1.434(4)
	Angles (deg)	
Mn−C16−C18	116.4(2)	122.6(3)
C8−C16−C18	120.2(2)	115.9(2)
C8−C16−O5	111.4(2)	110.4(2)
C18−C16−O5	111.0(2)	106.7(2)
C1−Cr−C2	83.1(1)	88.6(1)
C1−Cr−C3	84.8(1)	89.7(1)
C2−Cr−C3	90.2(1)	84.3(1)
C24−Mn−C25	89.4(1)	84.9(1)
C25−Mn−C26	90.3(2)	85.7(1)
C24−Mn−C26	85.9(2)	97.4(1)
C16−Mn−N	85.79(9)	90.56(9)

(28) (a) Nishio, M.; Hirota, M.; Umezawa, Y. *The CH/π Interaction, Evidence, Nature and Consequences, Methods in Stereochemical Analysis*; Marchand, A. P., Ed.; Wiley-VCH: New York, 1998. (b) Umezawa, Y.; Tsuboyama, S.; Takahashi, H.; Uzawa, J.; Nishio, M. *Tetrahedron* **1999**, *55*, 10047.

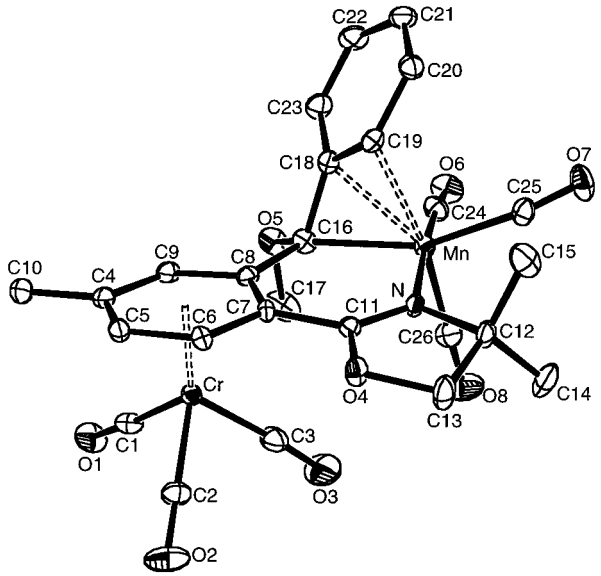

Figure 9. ORTEP diagram of the structure of **19**. Thermal ellipsoids are drawn at the 40% probability level. Hydrogen atoms have been omitted for clarity.

We first assumed that some molecular fluxionality was responsible for the low resolution of the measurements at room temperature. As low-temperature investigations did not improve at all the quality of the ^{1}H NMR spectra, we started to suspect the occurrence of radical species. ESR investigations of a frozen solution of **18** containing some amount of **19** in degassed $CDCl_3$ confirmed the presence of paramagnetic species, but the low resolution of the spectrum precluded any detailed interpretations. Nonetheless the signal observed at $g = 1.99$ suggests that the radical species is likely located at a carbon or/and a Mn(0) atom.[24] Difficulties arose when we attempted the ^{13}C NMR characterization of either **18** or **19**. With both complexes, taken as pure as possible, the resulting ^{13}C NMR spectra revealed the presence in solution of two different species, assumed to be **18** and **19**, in equal proportions and likely in equilibrium (eq 10).

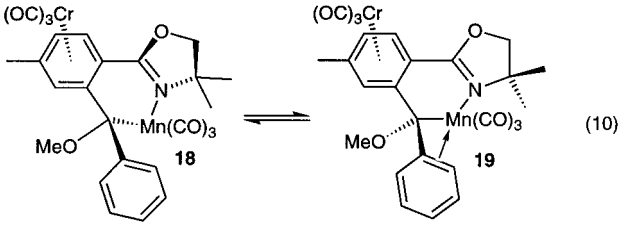

(10)

Two sets of poorly resolved ^{13}C signals produced by the $Cr(CO)_3$ and $Mn(CO)_3$ moieties of **18** and **19** could be detected in addition to the broad signals produced by the other parts of the molecules. Solution IR investigations of **18** and **19** afforded identical spectra, whereas KBr pellet samples afforded different patterns for each compounds. Thus in the solid state **18** produced a spectrum composed of two intense A bands at 2009 and 1958 cm^{-1} and two sets of E-bands with lifted degeneracy at 1936 and 1915 cm^{-1} ($Mn(CO)_3$) and at 1899 and 1880 cm^{-1} ($Cr(CO)_3$); complex **19** afforded a spectrum composed of two sets of CO stretching-mode bands at 2004 (A_1), 1933, 1900 cm^{-1} ($Mn(CO)_3$) and at 1957 (A_1), 1887 and 1877 cm^{-1} ($Cr(CO)_3$). The lability of **18** and **19** and the existence of radical species was further verified by submitting a mixture of the latter two to a treatment with *n*-Bu_3SnH in the presence of 2 equiv of PPh_3 in refluxing DME (eq 12). It is well established that *n*-Bu_3SnH possesses an affinity for radicals such as $^{\bullet}Mn(CO)_3L_2$ ($L = PR_3$).[29] According to analytical data, this experiment afforded one major product, **20**, which plausibly resulted from the coordination of PPh_3 to the Mn atom of either **18** or **19**, small amounts of *fac*-*n*-$Bu_3Sn{-}Mn(CO)_3(PPh_3)_2$ **21**, and **22**, which presumably arose from the quenching with *n*-Bu_3SnH of a biradical species formed upon homolytical cleavage of the $C_{benzyl}{-}Mn$ bond in **18** or **19** (eq 11). At this stage of our investigations the involvement of radical species in the interconversion process between **18** and **19** is still unclear.

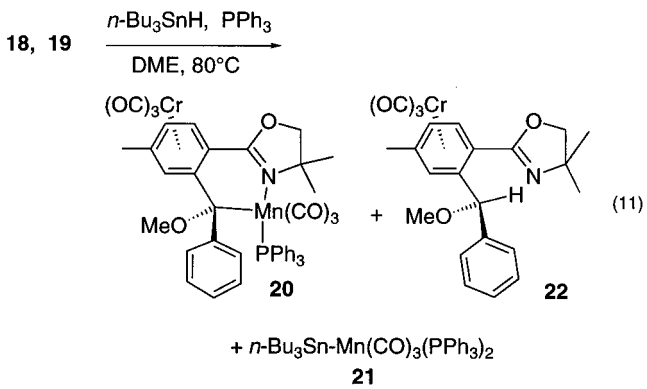

(11)

We nevertheless may state that the ready conversion of **18** into **19** and vice versa in solution is at least facilitated by the relative conformational flexibility of the 2-oxazolinyl heterocycle. To accommodate a $\eta^1{:}\eta^2$ coordination mode involving the Mn atom and the *endo*-phenyl group bonded to C16, the chelate must be able to absorb a part of the strains generated during the conversion of **18** into **19**. This is achieved mainly by slight distortions of the 2-oxazolinyl ring and a widening of the C16−Mn−N angle from 85.79(9)° in **18** to 90.56(9)° in **19** (Table 6). The distortions of the oxazolinyl ring are revealed by the deviations of atoms C13, O4, C11, N, and C12 from the corresponding least-squares mean planes, which are slightly larger in **19** as compared with **18** (Table 7).

Table 7. Deviations (Å) from the Least-Squares Mean-Plane Formed by Atoms C13, O4, C11, N, and C12 in Molecular Structures of Complexes 18 and 19

atom	**18**	**19**
C13	−0.0069	−0.097
O4	0.045	0.082
C11	0.001	−0.22
N	−0.034	−0.55
C12	0.058	0.091

Conclusion

The above-mentioned results establish the intermediacy of metal−carbene species and provide new information on the process of formation of spiralenes in the experimental conditions of the sequential reaction of RLi

(29) McCullen, S. B.; Brown, T. L. *J. Am. Chem. Soc.* **1982**, *104*, 7496.

Scheme 7

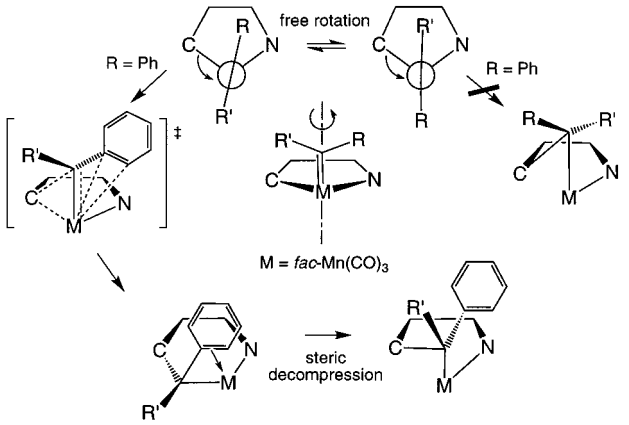

and MeOTf. The stereoselectivity of the *cis*-migration step that follows the formation of the metal−carbene intermediate is seemingly determined by two main factors. The first one is the relative flexibility of the organic chelating ligand that will determine the extent of the subsequent intramolecular structural rearrangements. The second one is the existence of an unsaturation at α,β positions with respect to the carbene carbon that will condition the degree of stereoselectivity of the *cis*-migration step. Notwithstanding the speculative intermetallic Cr−Mn (Re) interaction in the final bimetallic products, the *cis*-migration step should cause the Mn (Re) atom to formally "lose" two electrons in its valence shell and to adopt a formal 16-electron configuration upon conversion of the carbene intermediate into a Cr/Mn-spiralene.

Before the aryl ring moves from one of the equatorial positions of the Mn-centered octahedron to the carbene carbon, the carbene moiety may adopt only two conformations that are efficient for the optimal interaction between the vacant p-orbital of the carbene and the σ-orbital of the migrating arene carbon (Scheme 7). Given the octahedral geometry at the manganese atom and the obvious absence of steric strain for the free rotation of the carbene moiety around the $Mn-C_{carbene}$ axis, it is unlikely that the observed stereoselectivity of spiralene formation stems from the existence of a favored conformer of the transient carbene complex. Therefore, we may rely on Winstein−Holness and Curtin−Hammett considerations[8] to address the present mechanistic issues. Hence, a reasonable explanation for the observed stereoselectivity more probably lies in the intervention of a late transition state that prefigures an intermediate with a structure similar to that of **19** (Scheme 7). In such a case the Mn atom would circumvent the "loss" of two valence electrons formed during the *cis*-migration step by a stabilizing interaction with an adjacent two-electron ligand such as the Ph group attached to the former carbene carbon. This would allow a discrimination between the two carbene conformers by favoring the one in which the two-electron ligand, e.g., the phenyl group, is at an accessible position for the Mn center to interact with it. The formation of the $C_{Ar}-C_{benzyl}$ bond thus affords a strained and tense planar six-membered manganacyclic product which conformationally may stabilize itself by tilting the $Mn(CO)_3$ group toward the $Cr(CO)_3$ tripod. The structural change from a planar to a boatlike manganacycle is expected to be greatly favored with derivatives of 2-phenylpyridine, as the aromatic pyridyl ring is less flexible than an oxazolinyl. From these considerations, it appears that the putative intermetallic interactions between the Cr and Mn (Re) atoms as well as the intramolecular $\pi-\pi$ and CH/π interactions are not essential in the process of formation of *syn*-facial heterobimetallic complexes. The helicity coding[30] or directing effect[31] involved in the process leading to the organometallic spiralenes mainly arises from the constraints brought by the coordination modes of the chelated-Mn(0) center as well as from the nature of the chelating organic fragment.

The nature of the incidental intermetallic Cr−Mn interaction in Cr/Mn-spiralenes is currently being theoretically investigated and will be addressed in a future report. A reasonable part of the above discussion on the mechanism may likely be extrapolated to the Mn-spiralene case.

In conclusion we have further confirmed the intermediacy of metal carbene species in the process leading to heterobimetallic spiralenes (Scheme 8). We have found mechanistic evidence that rationalizes the peculiar selectivity observed in the formation of helical phenyl-substituted spiralenes (Scheme 8). The unprecedented fluxionality of the structurally flexible alkyl-substituted spiralenes has also attracted our attention (Scheme 8). The intermediacy of biradicals formed upon homolytic cleavage of the $C_{benzyl}-Mn$ bond has been partly evidenced and should be confirmed by further studies that will be carried out to clarify the influence of the benzylic carbon substituents over the homolytic $C_{benzyl}-Mn$ bond cleavage. In the future, we will concentrate our efforts in the development of the "spirogenic reaction" concept to the construction of elaborated polynuclear molecules having further applications in material sciences.

Experimental Section

All experiments were carried out under a dry atmosphere of argon with dry and degassed solvents. The acylrhenate anion PPN-**2** was synthesized by applying a published procedure.[10] Solutions of phenyllithium (1.8 M), *n*-butyllithium (1.8 M), and methyllithium (1.6 M) were purchased from Aldrich and Fluka companies. NMR spectra were acquired on Bruker DRX 500 and AC 300 spectrometers at room temperature unless otherwise stated. Chemical shifts were reported in parts per million downfield of Me_4Si. IR spectra were measured on a Perkin-Elmer FT spectrometer. Mass spectra were performed at the Service of Mass Spectrometry of University Louis Pasteur and at the Analytical Center of the Chemistry Institute of the University of Bonn. Elemental analyses (reported in % mass) were performed at the "Service Central d'Analyses du CNRS" and at the analytical center of the Charles Sadron Institute in Strasbourg. ESR experiments were carried out with a Bruker ESP 300 spectrometer at the Charles Sadron Institute in Strasbourg.

Experimental Procedure for the X-ray Diffraction Analysis of Compounds 4, 6a, 6b, 9, 18, and 19. Acquisition and processing parameters are displayed in Table 1. Reflections were collected on a KappaCCD diffractometer using Mo Kα graphite-monochromated radiation ($\lambda = 0.71073$ Å). The structure was solved using direct methods and refined against

(30) Ohkita, M.; Lehn, J. M.; Baum, G.; Fenske, D. *Chem. Eur. J.* **1999**, *5*, 3471.
(31) Katz, T. J. *Angew. Chem. Int. Ed.* **2000**, *39*, 1921.

Scheme 8

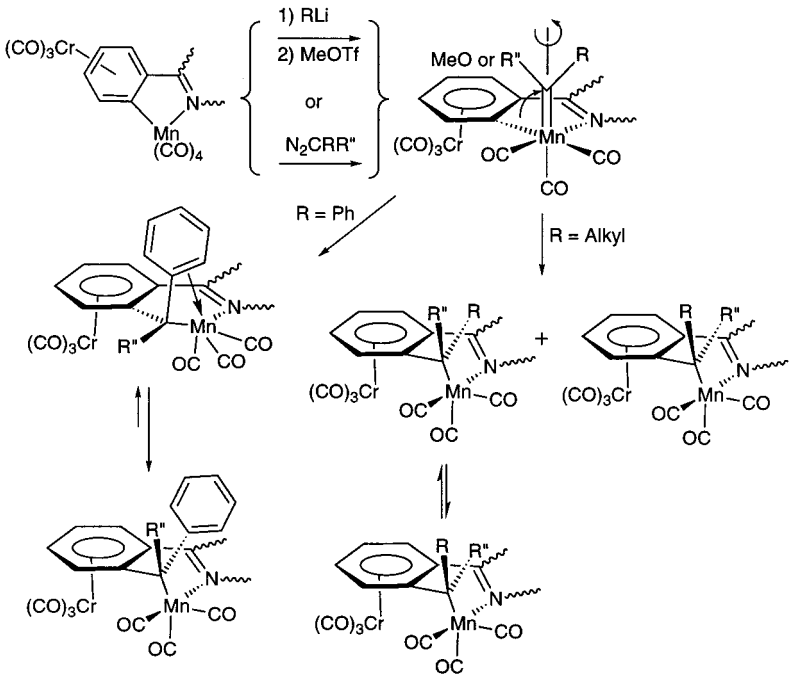

|*F*|. Hydrogen atoms were introduced as fixed contributors. For **9**, the absolute structure was determined by refining Flack's *x* parameter ($x = 0.03(3)$). For all computations the Nonius OpenMoleN package was used.[32]

Spectroscopic Detection of 3[33] by Low-Temperature ^{13}C NMR after O-Alkylation of PPN-2. To a solution of complex PPN-**2** in a NMR sample tube was added an excess of MeOTf at 203 K. The sample tube was then introduced in the NMR spectrometer and brought to 223 K. A total number of 8120 scans were acquired, and the ^{13}C NMR spectrum showed clearly after 78 min the signals of a unique reaction product, which was identified as carbene complex **3**. Warming the NMR sample tube to room temperature induced the formation of a new species identified as **4**. Complex **3**: ^{13}C-{^{1}H}NMR (CD_2Cl_2, 223 K, 125 MHz): δ 308.0 ((Ph)(MeO)C=Re), 231.4 ($Cr(CO)_3$), 197.3 (1C, Re−CO), 194.7 (2C, Re−CO), 150.0, 148.0, 146.0, 141.1, 138.0, 137.0, 129.4, 122.7, 120.1, 117.6, 115.1, 97.9, 94.1, 94.0, 92.0, 60.6 (MeO−$C_{carbene}$), 20.3 (Me_{py}).

Synthesis of 4. A solution of complex **1** (200 mg, 0.33 mmol) in 1,2-dimethoxyethane (15 mL) was cooled to −50 °C and added to a slight excess of PhLi (0.23 mL, 0.41 mmol, 1.8 M in hexane). The resulting greenish solution was stirred for 30 min and added to an excess of MeOTf (0.1 mL, 0.90 mmol), which caused the color of the mixture to turn to dark red. The mixture was warmed to room temperature in 6 h. The solvent was removed in vacuo and the oily residue dissolved in CH_2Cl_2. The solution was added to SiO_2 and evaporated to dryness under reduced pressure. The coated silica gel was loaded on top of a refrigerated column of SiO_2 packed in dry hexane. The separation was carried out by cooling the column at ca. 10 °C. Complex **4** was eluted with a mixture of hexane/CH_2Cl_2 (20:80) and the bright orange solution evaporated to dryness. The resulting solid (117.2 mg, 0.15 mmol, 51% yield) was hence recrystallized from a mixture of hexane and CH_2Cl_2 to afford yellow-orange crystals. Complex **4**: Anal. Calcd for $C_{26}H_{18}NO_7CrRe{\cdot}CH_2Cl_2$: C, 41.60; H, 2.59; N, 2.02. Found: C, 42.05; H, 2.45; N, 2.08. IR (CH_2Cl_2) ν(CO): 2015 (s), 1970(s), 1926 (vs), 1879 (vs) cm^{-1}. ^{1}H NMR ($CDCl_3$): δ 8.25 (d, 1H, H_{py}, $^3J = 5.2$ Hz), 7.33 (d, 1H, $H_{orthoPh-endo}$, $^3J = 7.4$ Hz), 7.21 (d, 1H, $H_{orthoPh-endo}$, $^3J = 7.2$ Hz), 7.14 (t, 1H, $H_{metaPh-endo}$, $^3J = 7.2$ Hz), 6.97 (m, 2H, H_{py}, $H_{paraPh-endo}$), 6.89 (t, 1H, $H_{metaPh-endo}$, $^3J = 7.5$ Hz), 6.69 (dd, 1H, H_{py}, $^3J = 5.5$ Hz, $^3J = 8.0$ Hz), 6.04 (t, 1H, $H_{metaArCr}$, $^3J = 6.1$ Hz), 5.38 (t, 1H, $H_{metaArCr}$, $^3J = 6.7$ Hz), 4.88 (d, 1H, $H_{orthoArCr}$, $^3J = 7.1$ Hz), 4.45 (dd, 1H, $H_{orthoArCr}$, $^3J = 6.3$ Hz, $^4J = 1.0$ Hz), 3.21 (s, 3H, *Me*O−C_{benzyl}), 1.81 (s, 3H, Me_{py}). ^{13}C{^{1}H} NMR ($CDCl_3$, 258 K): δ 233.9 (Cr−CO), 233.0 (Cr−CO), 227.8 (Cr−CO), 202.0 (Re−CO), 198.1 (Re−CO), 195.0 (Re−CO), 155.8, 151.4, 142.8, 140.5, 133.4, 132.7, 131.9, 129.1, 127.6, 126.8, 123.8, 98.8, 93.3, 92.4, 90.2, 89.7, 83.6, 78.4 (C_{benzyl}), 55.7 (MeO−C_{benzyl}), 20.2 (Me_{py}).

Synthesis of 6a and 6b. 5 (0.20 g, 0.42 mmol), *n*-BuLi (0.25 mL, 0.40 mmol), and MeOTf (0.10 mL, 0.90 mmol) were used, with 76% overall conversion (0.17 g). The crude mixture of **6a** and **6b** was separated by flash chromatography on SiO_2. Complex **6a** (64 mg, 37%) was eluted with a hexane/CH_2Cl_2 mixture (4:6). Complex **6b** (105 mg, 62%) was eluted with a hexane/CH_2Cl_2 mixture (3:7). Complex **6a**: Anal. Calcd for $C_{24}H_{22}NO_7CrMn$: C, 53.05; H, 4.08; N, 2.58. Found: C, 53.65;

(32) *Open Mole N. Interactive Structure Solution*; Nonius, B. V.: Delft, The Netherlands, 1997.

(33) Proposed systematic names for the compounds studied herein according to IUPAC recommendations for inorganic compounds: **3**, (OC-6-33) *exo*-(α-methoxybenzylidene)(tricarbonyl){3-methyl,2-[tricarbonyl(η^6-phenyl-$\kappa C^{2'}$)chromium], pyridine-κN}rhenium(I); **4**, [2-{2′,3′,4′,5′,6′-η^5-[1′(α-methoxybenzylidene-κC^{α})cyclohexadienyl-$\kappa C^{1'}$]-tricarbonylchromium},3-methylpyridine-κN] tricarbonylrhenium (Cr−Re); **6a**, [2-{2′,3′,4′,5′,6′-η^5-[1′((*exo*-α-methoxy)-*n*-pentylidene-κC^{α})-cyclohexadienyl-$\kappa C^{1'}$]tricarbonylchromium},3-methylpyridine-κN] tricarbonylmanganese (Cr−Mn); **8a**, [2-{2′,3′,4′,5′,6′-η^5-[1′((*exo*-α-methoxy)-*n*-pentylidene-κC^{α})cyclohexadienyl-$\kappa C^{1'}$]tricarbonylchromium},-pyridine-κN] tricarbonylmanganese (Cr−Mn); **9**, tricarbonyl[6-*n*-butyl,-{tricarbonyl{η^6-2′-[(*n*-butyl)(*exo*-methoxy)methylene-κC^{α}]phenyl}chromium},3-methyl,3,6-dihydropyridine-κN]manganese(I); **10a**, [2-{2′,3′,4′,5′,6′-η^5-{1′[(*exo*-α-methoxy)-*n*-ethylidene-κC^{α}]cyclohexadienyl-$\kappa C^{1'}$}tricarbonylchromium},pyridine-κN]tricarbonylmanganese (Cr−Mn); **11**, 4,4-dimethyl-2-[tricarbonyl(η^6-phenyl)chromium]-2-oxazoline; **12**, 4,4-dimethyl-2-[tricarbonyl(η^6-*para*-tolyl)chromium]-2-oxazoline; **13**, tetracarbonyl[4,4-dimethyl-2-{tricarbonyl(η^6-phenyl-$\kappa C^{2'}$)chromium}-2-oxazoline-κN]manganese(I); **14**, tetracarbonyl[4,4-dimethyl-2-{tricarbonyl(η^6-*para*-tolyl-$\kappa C^{2'}$)chromium}-2-oxazoline-κN]manganese(I); **15**, 4,4-dimethyl-2-[tricarbonyl(η^6-2′-acetylphenyl)chromium]-2-oxazoline; **16**, *fac*-tricarbonyl[4,4-dimethyl-2-{tricarbonyl(η^6-phenyl-$\kappa C^{2'}$)chromium}-2-oxazoline-κN](*exo*-triphenylphosphine)manganese(I); **17**, tricarbonyl[2-{tricarbonyl{η^6-2[(phenyl-$\kappa^2 C^{1'}C^{2'}$)phenylmethylene-κC^{α}]-phenyl}chromium}pyridine-κN]manganese(I); **18**, tricarbonyl[4,4-dimethyl-2{tricarbonyl{1′,2′,3′,4′,5′,6′-η^6-4′-methyl, 2′-[(α-*exo*-methoxy)-phenylmethylene-κC^{α}]phenyl}chromium},2-oxazoline]manganese(I); **19**, tricarbonyl[4,4-dimethyl-2{tricarbonyl{1′,2′,3′,4′,5′,6′-η^6-4′-methyl,2′-[(α-*exo*-methoxy)(phenyl-$\kappa^2 C^{1''}C^{2''}$)methylene-κC^{α}]phenyl}chromium}-2-oxazoline]manganese(I).

H, 4.31; N, 2.48. HRMS (EI) Calcd for $C_{24}H_{22}CrMnNO_7$: 543.0182. Found (deviation): 543.0175 (0.6 ppm). IR (CH_2Cl_2): ν(CO) 2005, 1955, 1921, 1888 cm^{-1}. ^1H NMR ($CDCl_3$): δ 7.78 (d, J = 5.4 Hz, 1H, H_{py}), 7.20 (d, J = 7.8 Hz, 1H, H_{py}), 6.69 (dd, ^3J = 7.8 Hz,^3J = 5.4 Hz, 1H, H_{py}), 6.16 (t, J = 6.0 Hz, 1H, H_{ArCr}), 4.91 (t, J = 7.6 Hz, 1H, H_{ArCr}), 4.18 (d, J = 6.2 Hz, 1H, H_{ArCr}), 4.11 (d, J = 7.8 Hz, 1H, H_{ArCr}), 3.67 (s, 3H, OMe), 3.15 (m, 1H, *n*-Bu), 2.19 (s, 3H, Me), 1.73 (m, 1H, *n*-Bu), 1.14 (m, 3H, *n*-Bu), 0.77 (t, J = 7.3 Hz, 3H, *n*-Bu), 0.52 (m, 1H, *n*-Bu) ppm. $^{13}C\{^1H\}$ NMR ($CDCl_3$, 258 K): δ 235.0 (3C, Cr−CO), 231.3 (1C, Mn−CO), 231.2 (1C, Mn−CO), 220.4 (1C, Mn−CO), 157.0, 151.0, 140.7, 129.5, 122.6, 94.4, 90.7, 88.2, 86.3, 84.6, 83.9, 78.0, 54.3 (OMe), 30.7 (1C, *n*-Bu), 30.0 (1C, *n*-Bu), 23.1 (1C, *n*-Bu), 19.8 (Me), 13.9 (1C, *n*-Bu) ppm. MS (EI): *m/e* 543.1 $[M]^+$, 487.1 $[M - 2CO]^+$, 459.1 $[M - 3CO]^+$, 375.1 $[M - 6CO]^+$, 320.1 $[M - 6CO - Mn]^+$, 286.1, 260.1, 248.0, 220.1, 194.1. Complex **6b**: Anal. Calcd for $C_{24}H_{22}NO_7CrMn$: C, 53.05; H, 4.08; N, 2.58. Found: C, 53.21; H, 4.37; N, 2.66. IR (CH_2Cl_2): ν(CO) 2005, 1954, 1921, 1894 cm^{-1}. ^1H NMR ($CDCl_3$): δ 7.74 (d, J = 5.3 Hz, 1H, H_{py}), 7.17 (d, J = 7.7 Hz, 1H, H_{py}), 6.60 (dd, ^3J = 7.9 Hz, ^3J = 5.4 Hz, 1H, H_{py}), 6.17 (t, J = 5.9 Hz, 1H, H_{ArCr}), 4.75 (t, J = 7.5 Hz, 1H, H_{ArCr}), 4.34 (d, J = 6.2 Hz, 1H, H_{ArCr}), 3.12 (d, J = 7.7 Hz, 1H, H_{ArCr}), 3.06 (s, 3H, OMe), 2.89 (m, 1H, *n*-Bu), 2.21 (s, 3H, Me), 1.82 (m, 1H, *n*-Bu), 1.66 (m, 1H, *n*-Bu), 1.40 (m, 2H, *n*-Bu), 0.96 (t, J = 7.3 Hz, 3H, *n*-Bu), 0.87 (m, 1H, *n*-Bu) ppm. $^{13}C\{^1H\}$ NMR ($CDCl_3$): δ 234.9 (3C, Cr−CO), 231.1 (1C, Mn−CO), 229.1 (1C, Mn−CO), 220.6 (1C, Mn−CO), 158.9, 150.2, 140.1, 127.6, 121.1, 98.5, 89.5, 87.7, 87.5, 87.1, 81.5, 75.4, 54.0 (OMe), 35.7 (1C, *n*-Bu), 28.6 (1C, *n*-Bu), 23.1 (1C, *n*-Bu), 20.0 (Me), 14.2 (1C, *n*-Bu) ppm.

Synthesis of 8a, and 8b. 7 (0.30 g, 0.66 mmol), *n*-BuLi (0.41 mL, 0.66 mmol), and MeOTf (0.15 mL, 1.36 mmol) were used, with 68% overall conversion (0.21 g). The mixture of two products was separated by flash chromatography on SiO_2. Complex **8a** (0.10 g) was eluted with a mixture of hexane/CH_2Cl_2 (4:6). Further elution with a hexane/CH_2Cl_2 mixture (4:6) yielded **8b** (0.11 g). Complex **8a**: Anal. Calcd for $C_{23}H_{20}CrMnNO_7$: C, 52.19; H, 3.81; N, 2.65. Found: C, 52.17; H, 4.23; N, 2.36. HRMS (EI) Calcd for $C_{20}H_{20}CrMnNO_4$ ($(M - 3CO)^+$): 445.0178. Found (deviation): 445.0173 (0.5 ppm). IR (CH_2Cl_2): ν(CO) 2006, 1957, 1923, 1888 cm^{-1}. ^1H NMR ($CDCl_3$): δ 7.89 (d, J = 5.4 Hz, 1H, H_{py}), 7.37 (t, J = 7.7 Hz, 1H, H_{py}), 6.83 (t, J = 6.6 Hz, 1H, H_{py}), 6.72 (d, J = 7.7 Hz, 1H, H_{py}), 6.23 (t, J = 6.0 Hz, 1H, H_{ArCr}), 5.01 (ddd,^3J = 7.5 Hz, ^3J = 6.1 Hz, ^4J = 1.2 Hz, 1H, H_{ArCr}), 4.23 (dd, ^3J = 6.1 Hz, ^4J = 1.2 Hz, 1H, H_{ArCr}), 4.16 (d, J = 7.5 Hz, 1H, H_{ArCr}), 3.68 (s, 3H, OMe), 3.19 (m, 1H, *n*-Bu), 1.69 (m, 1H, *n*-Bu), 1.15−0.8 (m, 3H, *n*-Bu), 0.75 (t, 3H, *n*-Bu), 0.70 (m, 1H, *n*-Bu) ppm. $^{13}C\{^1H\}$ NMR ($CDCl_3$, 258 K): δ 236.1 (3C, Cr−CO), 231.8 (1C, Mn−CO), 230.6 (1C, Mn−CO), 220.4 (1C, Mn−CO), 159.3, 153.1, 138.3, 123.7, 117.3, 92.9, 91.1, 90.3, 85.5, 83.7, 83.5, 77.9, 54.4 (OMe), 31.0 (1C, *n*-Bu), 29.9 (1C, *n*-Bu), 22.8 (1C, *n*-Bu), 14.3 (1C, *n*-Bu) ppm. MS (EI): *m/e* 529.0 $[M]^+$, 473.0 $[M - 2CO]^+$, 445.0 $[M - 3CO]^+$, 361.0 $[M - 6CO]^+$, 306.1 $[M - 6CO - Mn]^+$, 275.0, 234.0, 206.0, 180.1. Complex **8b**: HRMS (EI) Calcd for $C_{23}H_{20}CrMnNO_7$: 529.0025. Found (deviation): 529.0023 (0.2 ppm). IR (CH_2Cl_2): ν(CO) 2006, 1956, 1923, 1896 cm^{-1}. ^1H NMR ($CDCl_3$): δ 7.88 (d, J = 4.8 Hz, 1H, H_{py}), 7.35 (t, J = 7.7 Hz, 1H, H_{py}), 6.76 (t, J = 6.6 Hz, 1H, H_{py}), 6.70 (d, J = 7.7 Hz, 1H, H_{py}), 6.24 (t, J = 5.9 Hz, 1H, H_{ArCr}), 4.86 (t, J = 6.7 Hz, 1H, H_{ArCr}), 4.37 (d, J = 6.2 Hz, 1H, H_{ArCr}), 3.21 (d, J = 7.5 Hz, 1H, H_{ArCr}), 3.14 (s, 3H, OMe), 3.09 (m, 1H, *n*-Bu), 1.79 (m, 1H, *n*-Bu), 1.68 (m, 1H, *n*-Bu), 1.59 (m, 1H, *n*-Bu), 1.37 (m, 2H, *n*-Bu), 0.93 (t, J = 7.3 Hz, 3H, *n*-Bu) ppm. $^{13}C\{^1H\}$ NMR ($CDCl_3$, 258 K): δ 236.4 (1C, Cr−CO), 234.4 (1C, Cr−CO), 231.8 (1C, Cr−CO), 230.5 (1C, Mn−CO), 229.4 (1C, Mn−CO), 220.5 (1C, Mn−CO), 160.8, 152.5, 137.8, 122.3, 115.7, 96.4, 90.0, 89.4, 86.8, 86.6, 80.2, 75.6, 54.0 (1C, OMe), 36.0 (1C, *n*-Bu), 28.4 (1C, *n*-Bu), 23.1 (1C, *n*-Bu), 14.4 (1C, *n*-Bu) ppm. MS (EI): *m/e* 529.0 $[M]^+$, 473.0 $[M - 2CO]^+$, 445.0 $[M - 3CO]^+$, 361.0 $[M - 6CO]^+$, 306.1 $[M - 6CO - Mn]^+$, 274.0, 234.0, 206.0, 180.0.

Synthesis of 9. To a solution of complex **7** (200 mg, 0.44 mmol) in DME (10 mL) at −50 °C was added a solution of *n*-BuLi (0.55 mL, 0.88 mmol) in hexane. The resulting mixture was stirred 30 min and then added to MeOTf (0.19 mL, 1.76 mmol). The solution was slowly brought to room temperature within 5 h. The resulting solution was evaporated to dryness under reduced pressure, the residue redissolved in dry CH_2Cl_2, and SiO_2 added. The solvent was removed in vacuo and the coated silica gel loaded on top of a column packed with SiO_2 (60 μm) in dry distilled hexane. Complex **9** was eluted with a mixture of hexane and CH_2Cl_2 (3:7) and recovered as a black microcrystaline powder after removal of the solvents under reduced pressure (146 mg, 55%). Anal. Calcd for $C_{28}H_{32}NO_7CrMn$: C, 55.91; H, 5.32; N, 2.33. Found: C, 56.07; H, 5.14; N, 2.30. HRMS (FAB^+) Calcd for $C_{28}H_{32}NO_7CrMn$: 601.09643. Found (deviation): 601.09574 (1 ppm). IR (CH_2Cl_2) ν(CO): 2006, 1955, 1932, 1883 cm^{-1}. ^1H NMR ($CDCl_3$): δ 6.13 (t, 1H, H_{ArCr}), 5.66 (dd, 1H, H_{Hpy}), 5.39 (dd, 1H, H_{Hpy}), 4.94 (ddd, 1H, H_{ArCr}), 4.16 (dd, 1H, H_{ArCr}), 4.09 (dd, 1H, H_{ArCr}), 3.69 (s, 3H, *Me*O−), 3.47 (m, 1H), 2.35 (m, 2H), 1.93 (m, 2H), 1.5−0.8 (m, 18H). $^{13}C\{^1H\}$ NMR (CD_2Cl_2): δ 234.9 ($Cr(CO)_3$), 232.0 (Mn−CO), 230.5 (Mn−CO), 220.2 (Mn−CO), 177.2 (C═N), 128.5 (C_{Hpy}), 123.1 (C_{Hpy}), 90.4, 89.9, 88.5, 83.7, 83.0, 82.5, 79.3, 66.1 (C_6), 54.0 (MeO−), 36.3, 33.1, 30.5, 30.2, 28.5, 23.2, 22.4, 18.1, 14.3, 13.9. MS (FAB^+) *m/e*: 602.1 $[MH]^+$, 517.1 $[M - 3CO]^+$, 433.1 $[M - 6CO]^+$, 381.2 $[M - 6CO - Cr]^+$, 326.3 $[M - 6CO - Cr - Mn]^+$.

Synthesis of 10a and 10b. 7 (0.23 g, 0.50 mmol), MeLi (0.38 mL, 0.61 mmol), and MeOTf (0.10 mL, 0.90 mmol) were used, with 33% overall yield (72 mg). Flash chromatography on SiO_2 with a mixture of hexane/CH_2Cl_2 (4:6) at − 5 °C yielded **10a** (67 mg). Complex **10b** could be formed by allowing a solution of **10a** in CH_2Cl_2 to equilibrate at room temperature. Both complexes displayed sensitivity to air and a propensity to decompose after several hours spent in solution. Complex **10a**: Anal. Calcd for $C_{20}H_{14}CrMnNO_7$: C, 49.30; H, 2.90; N, 2.87. Found: C, 49.42; H, 3.08; N, 3.06. HRMS (EI) Calcd for $C_{20}H_{14}CrMnNO_7$: 486.9556. Found (deviation): 486.9561 (0.5 ppm). IR (CH_2Cl_2): ν(CO) 2008, 1958, 1925, 1890 cm^{-1}. ^1H NMR (C_6D_6): δ 7.39 (d, J = 5.5 Hz, 1H, H_{py}), 6.17 (td, ^3J = 7.8 Hz, ^4J = 1.4 Hz, 1H, H_{py}), 5.63 (t, J = 6.7 Hz, 1H, H_{py}), 5.44 (d, J = 7.7 Hz, 1H, H_{py}), 5.08 (t, J = 6.2 Hz, 1H, H_{ArCr}), 4.07 (d, J = 7.6 Hz, 1H, H_{ArCr}), 3.96 (t, J = 6.9 Hz, 1H, H_{ArCr}), 3.69 (s, 3H, OMe), 2.94 (dd, ^3J = 6.1 Hz, 4J = 1.2 Hz, 1H, H_{ArCr}), 1.75 (s, 3H, Me) ppm. Complex **10b**: ^1H NMR (C_6D_6): δ 7.33 (d, 1H, H_{py}), 6.28 (td, 1H, H_{py}), 5.68 (m, 2H, H_{py}), 5.10 (t, 1H,), 3.80 (t, 1H, H_{ArCr}), 3.11 (dd, 1H, H_{ArCr}), 2.91 (s, 3H, −OMe), 2.59 (d, 1H, H_{ArCr}), 2.03 (s, 3H, Me) ppm. MS (EI): *m/e* 487.0 $[M]^+$, 431.1 $[M - 2CO]^+$, 403.1 $[M - 3CO]^+$, 347.1 $[M - 5CO]^+$, 319.1 $[M - 6CO]^+$, 264.1 $[M - 6CO - Mn]^+$, 234.1, 206.0, 180.1. Due to equilibration between the two complexes, the ^{13}C NMR spectra could not be measured separately for **10a** and **10b** even at a lower temperatures. The following data are those obtained with the corresponding mixture. $^{13}C\{^1H\}$ NMR ($CDCl_3$, 258 K): δ 234.7 (Cr−CO), 231.8 (Mn−CO), 230.6 (Mn−CO), 230.5 (Mn−CO), 229.6 (Mn−CO), 221.2 (Mn−CO), 220.9 (Mn−CO), 160.6, 159.8, 153.5, 152.7, 138.9, 138.3, 124.0, 122.9, 118.1, 116.3, 98.0, 93.7, 91.6, 91.2, 91.0, 90.4, 87.3, 86.5, 85.8, 83.7, 83.3, 79.9, 79.0, 76.6, 54.9, 54.5, 23.0, 20.6 ppm.

Isomerization of Complex 8a in Complex 8b. A solution of complex **8a** in $CDCl_3$ was prepared in an NMR tube under an atmosphere of argon and degassed. The evolution of the composition of the solution was followed by acquiring a series of three free induction decays at t = 0, t = 24 h, and t = 48 h at 20 °C. Proportions in complexes **8a** and **8b** were calculated by comparison of the intensity of the methoxy group signal in **8a** (δ = 3.68 ppm) and the intensity of the methoxy group signal in **8b** (3.14 ppm). The same experiment was carried out by starting from a solution enriched in **8b**.

^1H NMR Monitoring of the Isomerization of 10a into 10b. A solution of complex **10a** (8.6 mg) and reference (1,3,5-

tris(terbutyl)benzene, 2.3 mg) in 0.75 mL of C_6D_6 was prepared in an NMR tube under a dry atmosphere of argon, degassed, and frozen. Scans were acquired on a Bruker AC300 spectrometer at 20 °C by using Bruker's software KINETICS. Chosen delays between recordings were the following: 20 spectra recorded with a 2 min delay, 10 spectra recorded with a 5 min delay, 6 spectra recorded with a 10 min delay, 9 spectra recorded with a 30 min delay, 9 spectra recorded with a 60 min delay. Calibration of the temperature was accomplished with a sample of ethylene glycol. The concentration in complex **10a** was calculated by comparison of the intensity of the methyl group signal (δ = 1.75 ppm) with that of the reference signal. For reaction times longer than 5 h, decomposition in the NMR sample tube precluded further investigations.

Preparation of 11.[34] $Cr(CO)_6$ (3.2 g, 14.5 mmol), 4,4-dimethyl-2-phenyl-2-oxazoline (2.5 g, 14.3 mmol), THF (15 mL), and DBE (150 mL) were refluxed for 36 h. Chromatography was performed on SiO_2/CH_2Cl_2; 77% yield (3.42 g). IR (CH_2Cl_2) ν(CO): 1975, 1898 cm^{-1}. ^1H NMR ($CDCl_3$): δ 5.96 (d, 2H, J = 5.6 Hz, H_{ArCr}), 5.36 (m, 3H, H_{ArCr}), 4.08 (s, 2H, $-O-CH_2$), 1.35 (s, 6H, Me). $^{13}C\{^1H\}$ NMR ($CDCl_3$): δ 231.5 (Cr−CO), 159.9 (C═N), 92.5 (C_{ArCr}), 92.1 ($2C_{ArCr}$), 91.5 (C_{ArCr}), 90.9 ($2C_{ArCr}$), 79.5, 67.9, 28.1 ($2CH_3$).

Preparation of 12. $Cr(CO)_6$ (2.4 g, 10.9 mmol), 4,4-dimethyl-2-*p*-tolyl-2-oxazoline (2-*p*-tolyl,4,4-dimethyl,3-aza,1-oxa,cyclopent-2-ene) (2.0 g, 10.6 mmol), THF (8 mL), and DBE (80 mL) were refluxed for 36 h. Chromatography was done on SiO_2/CH_2Cl_2:acetone (8:2); 44% yield (1.52 g). HRMS (FAB) Calcd for $C_{15}H_{15}NO_4Cr$: 325.040618. Found (deviation): 325.040920 (0.9 ppm). IR (CH_2Cl_2) ν(CO): 1972, 1894 cm^{-1}. ^1H NMR ($CDCl_3$): δ 6.02 (d, 2H, J = 6.0 Hz, H_{ArCr}), 5.15 (d, 2H, J = 6.0 Hz, H_{ArCr}), 4.04 (s, 2H, $-O-CH_2$), 2.20 (s, 3H, Me_{Ar}), 1.31 (s, 6H, $Me_{oxazoline}$) ppm. $^{13}C\{^1H\}$ NMR ($CDCl_3$): δ 231.0 ($Cr(CO)_3$), 159.7 (C═N), 109.5 (C_{ArCr}), 93.6 ($2C_{ArCr}$), 91.1 ($2C_{ArCr}$), 88.8 (C_{ArCr}), 79.4, 67.7, 28.1 ($2CH_3$), 20.5 (CH_3) ppm. MS (FAB$^+$): *m/e* 326.1 $[M + H]^+$, 269.2 $[M - 2CO]^+$, 241.2 $[M - 3CO]^+$, 190.2 $[MH - 3CO - Cr]^+$.

Synthesis of 13. Complex **11** (1.06 g, 3.4 mmol), $[Mn(CO)_5(PhCH_2)]$ (1.17 g, 4.1 mmol), and heptane (25 mL) were refluxed for 8 h. Chromatography was performed on SiO_2/hexane:CH_2Cl_2 (5:5); 96% yield (1.56 g). Anal. Calcd for $C_{18}H_{12}NO_8CrMn$: C, 45.30; H, 2.53; N, 2.93. Found: C, 44.95; H, 2.49; N, 2.84. IR (CH_2Cl_2) ν(CO): 2086, 2005, 1988, 1958, 1945, 1886 cm^{-1}. ^1H NMR ($CDCl_3$): δ 6.10 (d, 1H, J = 6.4 Hz, H_{ArCr}), 5.52−5.45 (m, 2H, H_{ArCr}), 5.24 (t, 1H, J = 6.1 Hz, H_{ArCr}), 4.52 (d, 1H, J = 8.5 Hz, $-O-CH_2$), 4.47 (d, 1H, J = 8.5 Hz, $-O-CH_2$), 1.47 (s, 3H, Me), 1.43 (s, 3H, Me). $^{13}C\{^1H\}$ NMR ($CDCl_3$): δ 234.6 (Cr−CO), 218.5 (Mn−CO), 213.7 (Mn−CO), 210.8 (Mn−CO), 209.4 (Mn−CO), 172.8 (C═N), 137.1, 106.8, 100.5, 93.7, 91.8, 88.7, 82.6, 66.8, 27.6 (Me), 27.2 (Me).

Synthesis of 14. Complex **12** (0.5 g, 1.5 mmol), $[Mn(CO)_5(PhCH_2)]$ (0.66 g, 2.3 mmol), and heptane (15 mL) were refluxed for 8 h. Chromatography was performed on SiO_2/hexane:CH_2Cl_2 (6:4); 86% yield (0.65 g). Anal. Calcd for $C_{19}H_{14}NO_8CrMn$: C, 46.45; H, 2.87; N, 2.85. Found: C, 46.49; H, 2.92; N, 2.82. IR (CH_2Cl_2): ν(CO) 2086.3, 2002.8, 1987.2, 1953.2, 1942.3, 1882.2 cm^{-1}. ^1H NMR ($CDCl_3$): δ 5.98 (d, 1H, ^4J = 1.0 Hz, H_{ArCr}), 5.54 (d, 1H, ^3J = 6.6 Hz, H_{ArCr}), 5.33 (dd, 1H, ^3J = 6.6 Hz, ^4J = 1.1 Hz, H_{ArCr}), 4.48 (d, 1H, ^3J = 8.5 Hz, $-O-CH_2-$), 4.43 (d, 1H, ^3J = 8.5 Hz, $-O-CH_2-$), 2.22 (s, 3H, Me), 1.45 (s, 3H, Me), 1.41 (s, 3H, Me). $^{13}C\{^1H\}$ NMR ($CDCl_3$): δ 234.5 (Cr−CO), 218.5 (Mn−CO), 213.6 (Mn−CO), 210.8 (Mn−CO), 209.3 (Mn−CO), 172.5 (C═N), 139.3, 108.3, 107.6, 98.4, 93.8, 89.6, 82.5, 66.7, 27.5 (Me), 27.3 (Me), 21.1 (Me).

Synthesis of 15. To a solution of **13** (0.20 g, 0.42 mmol) in dry DME (10 mL) was added MeLi (0.34 mL, 0.54 mmol) at −50 °C. The temperature of the reaction mixture was slowly raised to room temperature during 3 h. The color of the mixture changed from bright orange to deep red-brown. The reaction mixture was stirred overnight and the vessel opened to air. The brownish suspension that formed was filtered through a plug of Celite. The resulting solution was mixed with silica gel and the solvent removed under reduced pressure. The resulting coated silica gel was loaded on top of a silica gel column that was packed in hexane. Flash chromatography on SiO_2 and elution with a CH_2Cl_2/MeOH (98:2) mixture yielded an orange solution of complex **15** (80 mg, 54%). Anal. Calcd for $C_{16}H_{15}NO_5Cr$: C, 54.39; H, 4.28; N, 3.96. Found: C, 54.22; H, 4.33; N, 4.00. IR (CH_2Cl_2) ν(CO): 1983 (s), 1914 (s), 1654 (m) cm^{-1}. ^1H NMR ($CDCl_3$): δ 5.73 (d, 1H, ^3J = 6.4 Hz, H_{ArCr}), 5.47 (m, 2H, H_{ArCr}), 5.30 (t, 1H, ^3J = 6.1 Hz, H_{ArCr}), 4.10 (d, 1H, ^3J = 8.3 Hz, $O-CH_2-$), 4.05 (d, 1H, ^3J = 8.3 Hz, $O-CH_2-$), 2.51 (s, 3H, −C(O)Me), 1.36 (s, 3H, -Me), 1.33 (s, 3H, −Me). $^{13}C\{^1H\}$ NMR ($CDCl_3$): δ 230.6 (Cr−CO), 198.5 (−C(O)Me), 159.7 (C═N), 107.9 (C_{ArCr}), 92.1 (C_{ArCr}), 91.6 (C_{ArCr}), 90.3 (C_{ArCr}), 89.2 (C_{ArCr}), 80.0 ($O-CH_2$), 79.7 (C_{ArCr}), 68.6 ($-N-CMe_2$), 30.2 ($-C(O)Me$), 28.1 ($-N-CMe_2$), 27.9 ($-N-CMe_2$).

Synthesis of 16. Complex **13** (0.15 g, 0.31 mmol) and an excess of triphenylphosphine (0.25 g, 0.94 mmol) were dissolved in dry degassed heptane (10 mL) and brought to reflux during 5 h. The resulting red solution was stripped of solvent, the resulting residue dissolved in CH_2Cl_2, and silica gel added. The solvent was evaporated under reduced pressure and the coated silica gel loaded on top of a SiO_2 column packed in hexane. Chromatography on SiO_2/hexane:CH_2Cl_2 (6:4) yielded an orange-red complex (77%, 0.17 g). Anal. Calcd for $C_{35}H_{27}NO_7CrMnP\cdot CH_2Cl_2$: C, 54.29; H, 3.67; N, 1.76. Found: C, 54.18; H, 3.85; N, 1.86. IR (CH_2Cl_2): ν(CO) 2015, 1955, 1896 cm^{-1}. ^1H NMR ($CDCl_3$): δ 7.31−7.26 (m, 15H, PPh_3), 5.85 (d, 1H, J = 6.3 Hz, H_{ArCr}), 5.25−5.18 (m, 2H, H_{ArCr}), 4.66 (td, 1H, ^3J = 6.0 Hz, ^4J = 1.5 Hz, H_{ArCr}), 4.34 (d, 1H, J = 8.3 Hz, $-O-CH_2$), 3.73 (d, 1H, J = 8.3 Hz, $-O-CH_2$), 1.41 (s, 3H, Me), 0.44 (s, 3H, Me). ^{31}P NMR ($CDCl_3$): δ 49.32 (s, 1P, PPh_3). $^{13}C\{^1H\}$ NMR ($CDCl_3$): δ 235.4 (Cr−CO), 223.7 (d, 1C, J = 21.4 Hz, Mn−CO), 219.4 (d, 1C, J = 16.3 Hz, Mn−CO), 216.9 (d, 1C, J = 24.4 Hz, Mn−CO), 172.4 (C═N), 151.2 (d, 1C, J = 20.6 Hz, $C_{ArCr-ipso}$), 133.6−133.3 (m, 9C, PPh_3), 129.9 (s, 3C, PPh_3), 128.3 (d, 6C, J = 8.1 Hz, PPh_3), 107.8, 101.8, 93.6, 90.1, 87.1, 81.8, 67.7, 29.2 (Me), 24.0 (Me).

Synthesis of 17. Compound **13** (97 mg, 0.20 mmol) and $N_2{=}CPh_2$ (120 mg, 0.60 mmol) were dissolved in dry and degassed heptane. The mixture was then brought to reflux for 1 h until a reddish precipitate appeared. An additional amount of $N_2{=}CPh_2$ (120 mg, 0.60 mmol) was added to the medium, and the suspension was refluxed for additional 30 min. The reaction mixture was then cooled to room temperature and the solvent evaporated under reduced pressure to afford a solid. The latter was dissolved in CH_2Cl_2, and SiO_2 was added. The solvent was evaporated in vacuo and the coated silica gel loaded on top of a SiO_2 column packed in hexane. Chromatography on SiO_2 and elution with a hexane/CH_2Cl_2 mixture (5:5) yielded an orange-red complex (69%, 85 mg). Anal. Calcd for $C_{30}H_{22}NO_7CrMn\cdot 1/4CH_2Cl_2$: C, 57.07; H, 3.56; N, 2.20. Found: C, 56.91; H, 3.60; N, 2.20. HRMS (FAB$^+$) Calcd for $C_{27}H_{22}CrMnNO_4$ ($[M - 3CO]^+$): 531.033439. Found (deviation): 531.033147 (0.3 ppm). IR (CH_2Cl_2) ν(CO): 2004, 1985, 1903 (broad) cm^{-1}. ^1H NMR ($CDCl_3$): δ 8.18 (br, 1H), 7.73 (d, 1H, J = 7.6 Hz), 7.62 (br, 2H), 7.41 (t, 1H, J = 6.8 Hz), 7.29 (t, 1H, J = 7.3 Hz), 7.21−7.08 (m, 2H), 6.61 (d, 1H, J = 7.6 Hz), 5.97 (d, 1H, J = 6.6 Hz, H_{Ar}), 5.79 (br, 1H), 5.43 (t, 1H, J = 6.5 Hz, H_{Ar}), 5.30 (t, 1H, J = 6.2 Hz, H_{Ar}), 5.20 (d, 1H, J = 7.1 Hz, H_{Ar}), 4.22 (d, 1H, J = 8.3 Hz, $-O-CH_2-$), 3.72 (d, 1H, J = 8.3 Hz, $-O-CH_2-$), 1.13 (s, 3H), 0.54 (s, 3H). $^{13}C\{^1H\}$ NMR ($CDCl_3$, T = 263 K): δ 232.5 (Cr−CO), 229.5 (Mn−CO), 220.4 (Mn−CO), 220.2 (Mn−CO), 163.8 (C═N), 147.7, 137.4, 135.7, 132.1, 130.6, 129.4, 128.7, 128.2, 126.8, 126.0, 123.5, 116.7, 94.9, 94.4, 93.9, 93.5, 88.1, 87.8, 79.5, 71.3, 61.4, 26.8 ($N-CMe_2$), 25.1 ($N-CMe_2$). MS

(34) Kündig, E. P.; Ripa, A.; Liu, R.; Amurrio, D.; Bernardinelli, G. *Organometallics* **1993**, *12*, 3724.

(FAB$^+$): *m/e* 615.1 [M]$^+$, 531.1 [M − 3CO]$^+$, 504.1[M − 4CO + H]$^+$, 395.1 [M − 6CO − Cr]$^+$, 341.2 [M − 6CO − Cr − Mn]$^+$.

Preparation of 18, and 19. 14 (0.20 g, 0.41 mmol), PhLi (0.25 mL, 0.45 mmol), MeOTf (0.07 mL, 0.63 mmol) were used. Chromatography of the crude mixture on silica gel afforded after elution with a hexane/CH_2Cl_2 mixture (4:6) a 10:1 mixture of the two complexes **18** and **19**, respectively (0.16 g, 67% overall conversion). Careful recrystallization in a mixture of CH_2Cl_2/hexane at −18 °C allowed the isolation of pure samples of complexes **18** (dark brown crystals) and **19** (orange crystals). Complex **18**: Anal. Calcd for $C_{26}H_{22}CrMnNO_8$: C, 53.33; H, 3.80; N, 2.40. Found: C, 53.46; H, 3.82; N, 2.34. HRMS (FAB$^+$) Calcd for $C_{26}H_{22}CrMnNO_8$: 583.013098. Found (deviation): 583.012911 (0.3 ppm). IR (CH_2Cl_2): ν(CO) 2011, 1963, 1926, 1892 cm^{-1}. IR (KBr) ν(CO): 2009, 1958, 1936, 1915, 1899, 1880 cm^{-1}. MS (FAB$^+$): *m/e* 583.2 [M]$^+$, 499.2 [M − 3CO]$^+$, 415.2 [M − 6CO]$^+$, 361.2 [MH − 6CO − Mn]$^+$. Complex **19**: HRMS (FAB$^+$) Calcd for $C_{26}H_{22}CrMnNO_8$: 583.013098. Found (deviation): 583.012466 (1.1 ppm). IR (CH_2Cl_2) ν(CO): 2010, 1964, 1926, 1893 cm^{-1}. IR (KBr) ν(CO): 2004, 1957, 1933, 1900 (sh), 1887, 1877 cm^{-1}. MS (FAB$^+$): *m/e* 583.2 [M]$^+$, 499.2 [M − 3CO]$^+$, 415.2 [M − 6CO]$^+$, 364.5 [M − 6CO − Cr + H]$^+$, 308.3 [M − 6CO − Cr − Mn]$^+$.

Reaction of 18 and 19 with *n*-Bu_3SnH and PPh_3. A mixture of **18** and **19** (82 mg, 0.14 mmol) was dissolved in DME (20 mL) and added with *n*-Bu_3SnH (0.08 mL, 0.28 mmol) and PPh_3 (120 mg, 0.46 mmol). The solution was then brought to reflux during 10 min, allowed to cool to room temperature, and stirred overnight. The color of the solution changed from dark brown to bright red. The mixture was then stripped of solvents and the solid residue redissolved in CH_2Cl_2. The solution was added with SiO_2 and evaporated to dryness under reduced pressure. The resulting coated silica gel was loaded on top of a SiO_2 column packed in hexane under argon and cooled to 5 °C. Complex **21** was eluted with a mixture of 10% CH_2Cl_2 in hexane and recovered after removal of the solvents as a pale yellow solid (10 mg, 7.5% yield). Complex **20** was eluted with a mixture of 50% CH_2Cl_2 in hexane and recovered as an orange powder after removal of the solvents (64 mg, 54%). Complex **22** was eluted with a mixture of 80% CH_2Cl_2 in hexane and recovered as a yellow oily residue after removal of the solvents (less than 10 mg). Complex **20**: Anal. Calcd for $C_{44}H_{37}NO_8PCrMn\cdot 1/2CH_2Cl_2$: C, 60.21; H, 4.26; N, 1.66. Found: C, 60.74; H, 4.37; N, 1.52. HRMS (FAB$^+$) Calcd for $C_{44}H_{37}NO_8PCrMn$: 845.10424. Found (deviation): 845.10436 (0.1 ppm). IR (CH_2Cl_2) ν(CO): 2012, 1947, 1894, 1876 cm^{-1}. ^{1}H NMR ($CDCl_3$): δ 7.54 (t, 2H, ^3J = 7.3 Hz, Ph), 7.47 (t, 1H, ^3J = 7.4 Hz, Ph), 7.29 (m, 5H, Ph + PPh_3), 7.13 (t, 6H, ^3J = 7.5 Hz, PPh_3), 6.96 (t, 6H, ^3J = 8.8 Hz, PPh_3), 5.73 (m, 1H, Ar_{Cr}), 5.68 (m, 1H, Ar_{Cr}), 5.58 (s, 1H, Ar_{Cr}), 4.35 (d, 1H, ^2J = 8.0 Hz, −CH_2−O−), 3.57 (d, 1H, ^2J = 8 Hz, −CH_2−O−), 3.42 (s, 3H, MeO−), 1.92 (s, 3H, *p*-Me−Ar_{Cr}), 1.34 (s, 3H, −(*Me*)$_2$C−O−), −0.04 (s, 3H, −(*Me*)$_2$C−O−). ^{31}P NMR ($CDCl_3$): δ 50.7. ^{13}C{^{1}H} NMR ($CDCl_3$, 283 K): δ 235.3 (Cr(*C*O)$_3$), 224.3 (d, J_{C-P} = 14.4 Hz, Mn−*C*O), 219.2 (d, J_{C-P} = 11.4 Hz, Mn−*C*O), 216.3 (d, J_{C-P} = 15.1 Hz, Mn−*C*O), 172.7, 156.0, 155.9, 141.7, 133.9, 133.7, 133.4 (d, 6C, J_{C-P} = 5.3 Hz, PPh_3), 129.9 (3C, PPh_3), 128.8, 128.7 (d, 3C, J_{C-P} = 23.5 Hz, PPh_3), 128.2 (d, 6C, J_{C-P} = 4.5 Hz, PPh_3), 109.4, 108.3, 106.5, 95.3, 91.1, 81.3, 79.9, 67.2, 57.6, 29.1, 22.3, 21.3. MS (FAB$^+$): *m/e* 845.0 [M]$^+$, 761.0, 677.1, 625.1, 611.0, 527.0, 499.0, 415.0. Complex **21**: HRMS (FAB$^+$) Calcd for $C_{51}H_{57}P_2O_3Mn^{120}Sn$: 954.21854. Found (deviation): 954.21845 (0.1 ppm). IR (CH_2Cl_2) ν(CO): 1958 (m), 1877 (s) cm^{-1}. ^{1}H NMR (C_6D_6): δ 7.85 (m, 12H, PPh_3), 7.11−6.95 (m, 18H, PPh_3), 1.61 (m, 6H, PPh_3), 1.39 (m, 6H, *n*-Bu), 1.07−0.93 (m, 30H, *n*-Bu). ^{31}P NMR (C_6D_6): δ 75.5. MS (FAB$^+$): *m/e* 954.1 [M]$^+$, 897.0 [M − *n*-Bu]$^+$, 663 [M − *n*-Bu_3Sn − H]$^+$, 579 [M − *n*-Bu_3Sn − H − 3CO]$^+$, 374 [M − *n*-Bu_3Sn − CO − PPh_3]$^+$, 318 [M − *n*-Bu_3Sn − 3CO − PPh_3]$^+$. Complex **22**: IR (KBr) ν(CO): 1956, 1883 cm^{-1}. ^{1}H NMR (CD_2Cl_2): δ 7.50−6.90 (m, 5H, Ph), 6.37 (m, 1H, Ar_{Cr}), 5.98 (s, 1H, Ar_{Cr}), 5.86 (d, 1H, ^2J = 6.6 Hz, −CH_2−O−), 5.71 (m, 1H, Ar_{Cr}), 5.02 (d, 1H, ^2J = 6.6 Hz, −CH_2−O−), 3.89 (s, 1H, −CH(Ph)(OMe)), 3.28 (s, 3H, MeO−), 2.18 (s, 3H, *p*-Me−Ar_{Cr}), 1.47 (s, 3H, −(Me)$_2$C−), 1.06 (s, 3H, −(Me)$_2$C−). ^{13}C{^{1}H} NMR (278 K, $CDCl_3$): δ 232.3 (s, Cr(*C*O)$_3$), 160.1, 140.4, 128.2, 115.7, 115.3, 114.1, 109.9, 95.8, 89.9, 88.3, 86.9, 79.0, 78.9, 67.4 (MeO−), 57.0 (−CH_2O−), 28.1 (*Me*$_2$C), 20.9 (*Me*$_2$C). MS (FAB$^+$): *m/e* 446.2 [MH]$^+$, 414.1 [MH − CH_3OH]$^+$, 391.3 [MH − 2CO]$^+$, 361.2 [M − 3CO]$^+$, 310.2 [MH − 3CO − Cr]$^+$.

Acknowledgment. We thank the Deutscher Akademischer Austauschdienst (DAAD), the Deutsche Forchung Gemeinschaft (DFG), the Alexander von Humboldt Foundation (AvH Stiftung), and the Centre National de la Recherche Scientifique (CNRS) for supporting this work. We gratefully acknowledge the assistance provided by Ulrike Weynand (Kekulé Institut-Bonn) for the ^{13}C NMR low-temperature experiments and thank Rouben Allagapen (Strasbourg) for his contribution to this work.

Supporting Information Available: ESR spectra of compounds **8a** and **18**, tables of crystal data, and complete lists of structural information for compounds **4**, **6a**, **6b**, **9**, **18**, and **19** (refined atomic coordinates, anisotropic thermal parameters, interatomic distances and angles). This material is available free of charge via the Internet at http://pubs.acs.org.

OM0006920